# Durham E-Theses

## The influence of elevated CO2 on NF-kappaB pathway activation

SMITH, ZOE,LYNN

**How to cite:**

SMITH, ZOE,LYNN (2019) *The influence of elevated CO2 on NF-kappaB pathway activation* , Durham theses, Durham University. Available at Durham E-Theses Online: http://etheses.dur.ac.uk/13428/

**Use policy**

# The influence of elevated CO$_2$ on NF-κB pathway activation

Zoe Lynn Smith

This thesis is submitted for the degree of
Master of Research

Department of Biosciences
Durham University
2019

# Abstract

Carbon dioxide ($CO_2$) makes up 0.04% of the earth's atmosphere and plays a vital role in many biological processes, including photosynthesis and respiration. Abnormal elevations in $CO_2$ levels (hypercapnia) within the body can be pathogenic or medically induced (termed permissive hypercapnia). Permissive hypercapnia has been found to improve the morbidity and mortality rates of patients suffering from Acute Respiratory Distress Syndrome (ARDS). This has led to the discovery that hypercapnia acidosis potentially reduces both lung injury and NF-κB induced inflammation. $CO_2$ is hydrated into carbonic acid by the enzyme carbonic anhydrase, which spontaneously dissociates into bicarbonate and hydrogen ions. Therefore, when $CO_2$ increases there is also an increase in hydrogen ions, causing an acidosis. There is conflicting evidence which indicates that both the elevations in $CO_2$ and secondary pH reductions are the primary cause for attenuating NF-κB activation. Evidence from this thesis would indicate that both elevated $CO_2$ and reductions in pH, via different mechanisms, reduces NF-κB activation within the NF-κB/293/GFP/Luc™ reporter cell line.

$CO_2$ is normally an inert gas but under physiological conditions $CO_2$ can interact with neutral amines to form carbamates. Recent advancements in trapping this highly labile interaction, has led to the discovery of carbamate formation at K48 of ubiquitin. Ubiquitin can form chains which tag proteins, and K48 linked polyubiquitin chains signal for protein degradation via the 26S proteasome. NF-κB activation requires the degradation of the inhibitor, IκBα, via K48 polyubiquitin tagging. It is therefore hypothesised that hypercapnia reduces NF-κB activation via carbamylation of K48. This would then prevent K48 polyubiquitination and the breakdown IκBα. Evidence from this thesis confirms the importance of K48 linked ubiquitin for NF-κB activation, and provides compelling evidence that hypercapnia acts via reducing K48 polyubiquitination.

## Declaration

The work presented in this thesis was carried out at Durham University between October 2018 and July 2019. The work is my own original research unless otherwise indicated by statement or citation. This work has not been submitted for any other qualification.

## Statement of Copyright

## Acknowledgements

# Table of Contents

# List of Figures

**Figure 3.14** Transfection with K63R ubiquitin mutant significantly reduced NF-κB activation, but the effect of elevated CO$_2$ was lost

## List of Tables

# List of Abbreviations

A549 – Human Adenocarcinoma Alveolar Basal Epithelial Cells

AIC – Akaike Information Criterion

ALI – Acute Lung Injury

ARDS – Acute Respiratory Distress Syndrome

Arg - Arginine

Asp –  Aspartic Acid

ATP – Adenosine Triphosphate

BALF – Bronchoalveolar Lavage Fluid

BEAS-2B – Bronchial Epithelial transformed with Ad12-SV40 2B

BSA – Bovine Serum Albumin

$Ca^{2+}$ - Calcium Ion

cIAP – Cellular Inhibitor of Apoptosis

$CO_2$ – Carbon Dioxide

Cx – Connexin

DMEM – Dulbecco's Modified Eagle Medium

DMSO – Dimethyl Sulfoxide

DUB – Deubiquitinase

ELISA - Enzyme-Linked Immunosorbent Assay

FBS – Fetal Bovine Serum

GFP – Green Fluorescent Protein

Glu – Glutamic Acid

Gly – Glycine

$H^+$ - Hydrogen ion/Proton

$H_2O$ - Water

$H_2O_2$ – Hydrogen Peroxide

Hb – Haemoglobin

HBE – Human Bronchial Epithelial Cells

HEK 293 – Human Embryonic Kidney Cells 293

HPAEC – Human Pulmonary Artery Endothelial Cells

HT-29 – Human Colon Cancer Cells

IκB – Nuclear Factor kappa-light-chain-enhancer of Activated B Cells Inhibitor

IKK - IκB Kinase

IL – Interleukin

J774 – Mouse Macrophages

K – Lysine

LB – Luria Broth

LPS – Lipopolysaccharides

Luc signal – Luciferase Signal

M1 – Methionine linked ubiquitin

mCMV – Minimal Cytomegalovirus

MCP – Monocyte Chemoattractant Protein

MEF – Mouse Embryonic Fibroblast

$Mg^{2+}$ - Magnesium Ion

mRNA – Messenger Ribonucleic Acid

NEMO – NF-κB Essential Modulator

NF-κB – Nuclear Factor kappa-light-chain-enhancer of Activated B Cells

NIK – NF-κB-induced Kinase

$O_2$ – Oxygen

PenStrep – Penicillin-Streptomycin Antibiotic

PBMC – Peripheral Blood Mononuclear Cells

PBS – Phosphate Buffered Saline

Phe - Phenylalanine

PTM – Post-Translational Modification

R – Arginine

RHD – REL-homology Domain

RIP – Receptor Interacting Protein

RuBisCo – Ribulose-1,5-Biphosphate Carboxylase Oxygenase

RuBP – Ribulose Bisphosphate

SAEC – Small Airway Epithelial Cells

TAD – Transactivation Domain

TEO – Triethyloxonium Tetrafluoroborate

THP-1 – Human Monocyte Cells

TLR – Toll-like Receptor

TMS-DAM - Trimethylsilyldiazomethan

TNF-$\alpha$ - Tumour Necrosis Factor $\alpha$

TNFR1 – Tumour Necrosis Factor Receptor 1

TRADD – TNF-Associated Protein with a Death Domain

TRAF – TNF Receptor Associated Factor

UBD – Ubiquitin Binding Domain

Val – Valine

VILI – Ventilator Induced Lung Injury

# 1 - Introduction

## 1.1 Carbon Dioxide

Over the course of history the level of carbon dioxide ($CO_2$) within the atmosphere has fluctuated from around 284 to 6000 ppmv over the last 600 or so million years (Taylor and Cummins, 2011). Through a complex long-term $CO_2$ feedback system involving longer term factors like weathering, to shorter term influences like stomatal density, the level of $CO_2$ has been kept within a finite range (Beerling and Berner, 2005). Current atmospheric levels are around 400 ppmv (corresponding to 0.04%), which has increased roughly 40% since the pre-industrial mid 1800's (Taylor and Cummins, 2011; McGee, 2015). The biological effects of $CO_2$ ranges from protein modifications that alter function, to influencing whole organism behaviour (Cummins *et al.*, 2014). In this study we will be focusing on the effects of increasing $CO_2$ on the NF-κB (Nuclear factor kappa-light-chain-enhancer of activated B cells) pathway and polyubiquitin formation.

## 1.2 $CO_2$ within the body and effects on pH

$CO_2$ is a waste product from oxidative respiration, with humans producing approximately 20 moles of $CO_2$ per day (Meigh *et al.*, 2013). This elevates the $CO_2$ levels within the body to around 5% or 35-45 mmHg, which is termed normocapnia. In the body $CO_2$ is hydrated by water to form carbonic acid, a reaction catalysed by the zinc-containing metalloenzyme, carbonic anhydrase. This enzyme drastically increases the rate of an ordinarily slow reaction, with a rate constant of $10^{-5}$-$10^{-6}$ per second (Lindskog and Coleman, 1973). Carbonic acid rapidly dissociates into bicarbonate and protons ($H^+$) (see Figure 1.1). The bicarbonate is then carried around the body bound to haemoglobin (Hb), plasma proteins or dissolved within the blood (Curley, Laffey and Kavanagh, 2010). This system acts like a buffer within the body, with the pH related to the concentration of $CO_2$ and bicarbonate according to the Henderson-Hasselbalch equation (Abolhassani *et al.*, 2009).

The presence of carbonic anhydrase within mammalian systems means that as $CO_2$ levels increase, there is an increase in $H^+$, causing an alteration in pH. For example, the pH of media on the human colon cancer HT-29 cells treated with 5%, 10% and 15% $CO_2$ over 48 hours, dropped from a physiological pH 7.3 to 6.9-6.7 (Abolhassani et al., 2009). Therefore, whenever an effect is seen by alterations in $CO_2$, pH must also be controlled or considered as a potential causal factor.

$$\text{Carbonic Anhydrase}$$

$$CO_2 + H_2O \rightleftharpoons H_2CO_3 \rightleftharpoons HCO_3^- + H^+$$
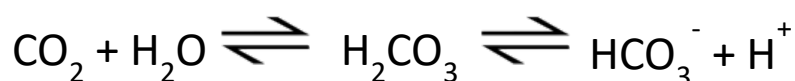
**Figure 1.1**
Reaction showing the hydration of carbon dioxide into carbonic acid via the metalloenzyme, carbonic anhydrase. The carbonic acid then dissociates into bicarbonate and protons.

Changes in $CO_2$ and pH levels are sensed by neurones called chemoreceptors, found both centrally (within the brain stem) and peripherally (carotid body) (Curley, Laffey and Kavanagh, 2010). Elevations in $CO_2$ and $H^+$ are major stimuli for increasing ventilation, with a rise in $CO_2$ causing increases to both tidal volume and respiratory frequency. Multiple areas within the brain stem respond to alterations in $CO_2$, but other cells like renal proximal tubule cells can also respond to elevated $CO_2$ levels, by increasing bicarbonate reabsorption (Putnam, Filosa and Ritucci, 2004).

Physiologically $CO_2$ has a wide range of effects and these include increasing cardiac output, pulmonary vascular tone, cerebral blood flow, partial pressure of oxygen ($O_2$) in the blood and cerebral fluid, oxygenation of peripheral tissues, $O_2$ tension in subcutaneous tissues and causes a reduction in $O_2$ consumption in tissues (Curley, Laffey and Kavanagh, 2010). $CO_2$ is also implicated in suppressing immune responses and specifically the NF-κB pathway (O'Croinin et al., 2008; Cummins et al., 2010; Wang et al., 2010), which is of particular interest in this study.

## 1.3 Hypercapnia

Abnormally elevated $CO_2$ levels (hypercapnia) can be caused by factors like shivering, heat stroke, hyperpyrexia and neuroleptic malignant syndrome. However, the most common cause for increased $CO_2$ levels is medically induced, termed permissive hypercapnia (Curley, Laffey and Kavanagh, 2010). In the past, treatment of Acute Lung Injury (ALI) and Acute Respiratory Distress Syndrome (ARDS) involved normalising $O_2$ and $CO_2$ levels, but this would cause excessive cell stretch injury to bronchial and alveolar cells by activating the NF-κB pathway (Horie *et al.*, 2016). Therefore, lower tidal volumes were adopted as a treatment which significantly reduced mortality rates (The Acute Respiratory Distress Syndrome Network, 2000), but results in a secondary acidosis.

Interestingly, a recent meta-analysis study on ARDS patients from 40 countries and 1899 subjects, found that severe hypercapnia acidosis was independently associated with higher intensive care unit patient mortality (Nin *et al.*, 2017). This contradicts the previous notion that hypercapnia is neutral to overall patient morbidity and mortality. However, this study did not account for ARDS severity or lung compliance, both indications of lung injury severity. A separate investigation including these factors in their analysis, which contained a cohort of 415 patients with ARDS, found that severe $CO_2$ levels in the first 48 hours was not a predictor of mortality, but pH and ARDS severity were (Muthu *et al.*, 2017). It is possible these factors or potentially the lower cohort number account for the differing conclusions, but this does highlight the uncertainty of the overall effects of hypercapnia on the body.

## 1.4 Carbamylation

One of the first post-translational modifications (PTM) to be discovered was the addition of $CO_2$ (carbamylation) onto protein amino groups (Linthwaite *et al.*, 2018). Carbamylation involves the nucleophilic attack of the neutral amine on $CO_2$, converting it into an anionic amine (Lorimer and Miziorko, 1980). This can alter the electrostatic properties of proteins. Dissolved $CO_2$ can form adducts with the N-

terminal and ε-amino groups of amino acids, peptides and proteins (Terrier and Douglas, 2010). In an environment containing $CO_2$, carbamylation of the ε-amino group on lysine can occur spontaneously under basic conditions; and computational analysis indicates that 1.3% of larger proteins have the potential for lysine carbamylation (Jimenez-Morales *et al.*, 2014). Crystal structures of the following molecules have shown evidence of lysine carbamylation; urease, alanine racemase, transcarboxylase 5S, class D beta-lactamase and phosphotriesterase (Linthwaite *et al.*, 2018). Taking this together, carbamylation has the potential to be an important and widespread biological mechanism for protein control.

Carbamate formation is a relatively labile and readily reversible reaction (Terrier and Douglas, 2010), and studying carbamate formation outside the privileged cellular environment makes carbamylation a challenging modification to study (Linthwaite *et al.*, 2018). Techniques like electrospray ionisation mass spectrometry can demonstrate the presence of carbamates but cannot identify the specific locations of the modification (Terrier and Douglas, 2010). Similarly, alkylating carbamates with trimethylsilyldiazomethan (TMS-DAM) cannot be used to identify carbamates formed under physiological conditions, as the compound is insoluble in water (Ito and Ushitora, 2006; Linthwaite *et al.*, 2018). However, a method for trapping carbamates under physiological conditions was recently developed, involving the treatment of carbamates with triethyloxonium tetrafluoroborate (TEO). Carbamylation of the *α-N*-acetyl-lysine and the dipeptide Gly-Phe under an aqueous environment at a pH of 8.5, was demonstrated using this technique. TEO can also trap known and unknown carbamates on proteins within an aqueous solution and at a physiological pH (7.4), as well as trap $CO_2$ on whole cells (Linthwaite *et al.*, 2018). This technique therefore allows for easier identification of physiological carbamates, allowing to expand our knowledge of carbamates and their biological significance.

## 1.5 Known carbamylated proteins haemoglobin, RuBisCO and Connexin 26

Carbamylation is known to modulate the functions of Hb, ribulose-1,5-biphosphate carboxylase oxygenase (RuBisCo) and Connexin 26 (Cx26).

### 1.5.1 Haemoglobin

One of the first PTM's to be discovered was carbamylation of Hb, a protein responsible for the transport of $O_2$ around the body and is found within red blood cells. Human Hb contains two $\alpha$ and $\beta$ polypeptide chains bound to a haem group, with each haem containing a porphyrin ring and ferrous atom capable of reversibly binding 1 molecule of $O_2$. Bohr demonstrated that Hb has a sigmoidal curve for $O_2$ dissociation, indicative of its cooperative binding to $O_2$. Deoxyhaemoglobin is held by electrostatic interactions in the tense conformation, which has a low affinity for $O_2$. When $O_2$ binds to Hb, these electrostatic interactions are broken which allows the transformation into the relaxed conformation, increasing the affinity for $O_2$ by 500 times (Hsia, 2002). However, elevated $CO_2$ shifts the $O_2$ dissociation curve to the right, an effect called the Bohr shift, in which high $CO_2$ levels reduces Hb affinity for $O_2$, as shown in Figure 1.2 (Bohr, Hasselbalch and Krogh, 1904). This means that when blood passes through the tissue capillaries which have high $CO_2$ concentrations, the Hb offloads the $O_2$. The $CO_2$ binds to the Val-1$\beta$ on the $\beta$ chain (Matthew *et al.*, 1977), an alternative site to $O_2$ binding site and is an example of an allosteric interaction. Protons and red-cell 2,3-bisphosphoglycerate also allosterically alter the $O_2$ affinity of Hb (Hsia, 2002). Conversely, increasing $O_2$ levels at constant $CO_2$ concentrations causes an increase in $CO_2$ uptake by Hb (Christiansen, Douglas and Haldane, 1914).

Partial pressure $O_2$ (mmHg)
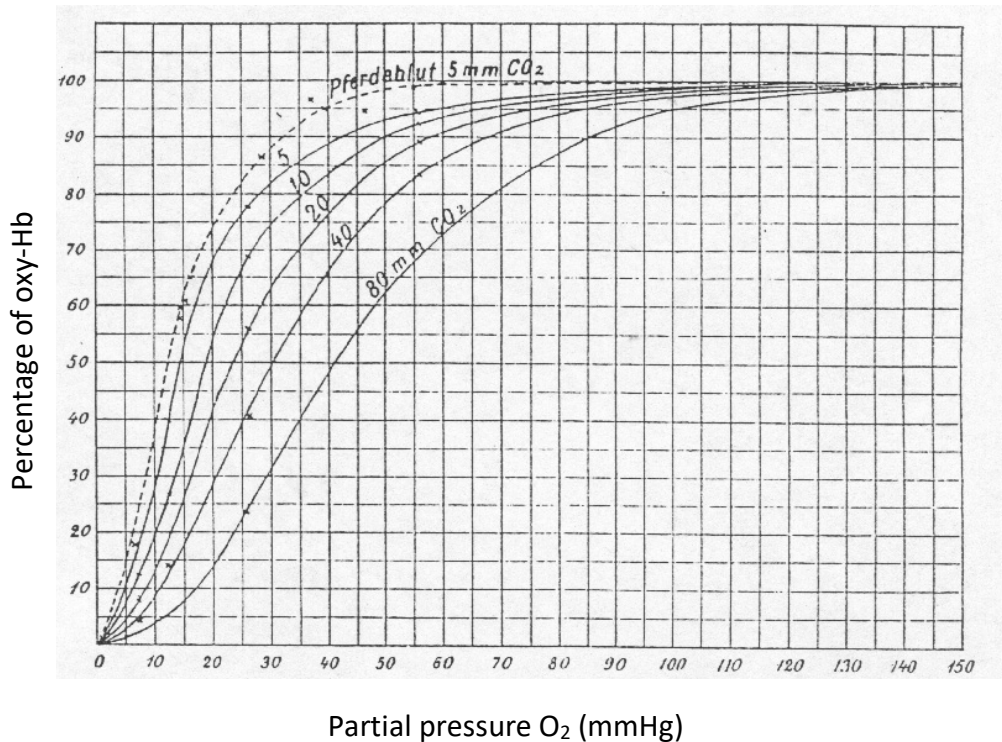
**Figure 1.2**
The Bohr Shift. Oxygen binding curves for dog Hb (solid lines) and horse Hb (dashed line) shift to the right with increasing partial pressures of $CO_2$ (5, 10, 20, 40 and 80 mmHg). Taken from (Bohr, Hasselbalch and Krogh, 1904).

### 1.5.2 RuBisCO

The photosynthetic enzyme RuBisCo is the most abundant protein on the planet, and one of the most extensively studied enzymes. $CO_2$ fixation was first described in photosynthesis in the 1950's. The enzyme catalyses the addition of $CO_2$ onto ribulose bisphosphate (RuBP), the key $CO_2$ fixation step within the Calvin cycle of photosynthesis (Yokota, 2017).

In the 70's it was discovered that there was a $CO_2$ activator site distinct from the $CO_2$ substrate binding site (Lorimer, 1979). The enzymatic activity of RuBisCo is dependent on $CO_2$ binding to the $\varepsilon$-amino group of K-201 to form a carbamyl anion, to which $Mg^{2+}$ interacts (Yokota, 2017). The complex is then stabilised by $Mg^{2+}$ interacting with the carboxylate groups of Asp-203 and Glu-204 and 3 water molecules. Upon substrate binding the water molecules are replaced, altering the structure of the active site (Taylor and Andersson, 1996) and allows the full activation

of RuBisCo. The rate of activation of RuBisCo is dependent upon the $CO_2$ concentration but independent of the $Mg^{2+}$ concentration. It was also demonstrated that the activation of the enzyme was increased under alkaline conditions (Lorimer, Badger and Andrews, 1976), highlighting the importance of pH for the activation of enzymes controlled by $CO_2$.

### 1.5.3 Connexin 26

Cx26 hemichannels contribute to the chemosensory control of breathing (Meigh *et al.*, 2013) and elevated $CO_2$ levels were demonstrated to modulate the function of the transmembrane gap junction *in vitro* and *in vivo* (Huckstepp *et al.*, 2010). Upon an increase in $CO_2$ there was a progressive increase in release of adenosine triphosphate (ATP) in the ventral medulla surface, where Cx26 channels are found. This release of ATP was independent of pH, bicarbonate production and extracellular $Ca^{2+}$ (Huckstepp *et al.*, 2010). Carbamylation of Cx26 at K-125 causes a salt bridge to form with the Arg104 residue on the neighbouring subunit. This results in the opening of the channel, preventing the closed formation of the channel forming and allowing the release of ATP. This sensitivity to $CO_2$ was also shown in Cx30 and Cx32, but not Cx31 (Meigh *et al.*, 2013).

## 1.6 NF-κB pathway

The NF-κB pathway is an essential modulator in coordinating inflammatory responses, innate and adaptive immunity, nucleosome remodelling, cellular differentiation, proliferation and apoptosis (Sun, 2011; Hayden and Ghosh, 2012; Mitchell, Vargas and Hoffmann, 2016). Aberrant NF-κB signalling has been linked to cardiovascular disease, autoimmune diseases, neurodegenerative diseases, cancer and diabetes (Hayden and Ghosh, 2012).

NF-κB signalling contains a family of 5 protein monomers, p65/RelA, RelB, cRel, p50 and p52, each with their own distinct function (Mitchell, Vargas and Hoffmann, 2016). These contain N-terminal REL-homology Domain's (RHD) to allow the

formation of homo- or heterodimers, which can then bind to κB elements found within enhancers and promoters on DNA. Only RelB, c-Rel and p65 contain C-terminal transactivation domains (TADs) that confer the ability to activate transcription, while the p50 and p52 subunits must dimerise with these to activate transcription. Alternatively, p50 and p52 can homodimerise and compete with TAD containing subunits for the κB sites on DNA (Hayden and Ghosh, 2012). The NF-κB pathway has over 150 target genes which include the inflammatory signals TNF-α, interleukin 6 (IL-6) and IL-8 (Pahl, 1999). NF-κB also stimulates the production of the inhibitory protein IκBα, which under non-stimulatory conditions inhibits the action of NF-κB dimers as part of a negative feedback loop for NF-κB activation (Chiao, Miyamoto and Verma, 1994).

There are two distinct NF-κB pathways, the canonical/classical and non-canonical/alternative. The canonical pathway is activated by inflammatory cytokines like TNF-α or toll-like receptor (TLR) ligands. After TNF-α binds to the TNF Receptor 1 (TNFR1) it trimerises and recruits the adaptor protein, TNF-associated protein with a death domain (TRADD). This then assembles a complex with the receptor interacting protein-1 (RIP1), cellular inhibitor of apoptosis 1 (cIAP1), cIAP2 and TNF receptor associated factor-2 (TRAF2). RIP1 is rapidly modified with polyubiquitin chains which recruit the IκB kinase (IKK) complex comprising of IKKα, IKKβ and NF-κB essential modulator (NEMO) (Wertz and Dixit, 2010). IKK is activated by phosphorylation which then phosphorylates IκBα. Under non-stimulated conditions the IκBα sequesters the NF-κB dimers within the cytoplasm ensuring they remain inactive. Upon phosphorylation of IκBα, it is ubiquitinated and degraded by the proteasomal system to release the NF-κB dimer subunits. This enables the NF-κB subunits to translocate to the nucleus and bind to target DNA (Iwai, 2012) (see Figure 1.3).

The alternative pathway is activated by ligands binding to TNF-receptor family proteins, including the lymphotoxin-β receptor and CD40. This stabilises NF-κB-inducing kinase (NIK), which under unstimulated conditions is ubiquitinated and

degraded. Once NIK is stable it phosphorylates the IKKα homodimer. This then phosphorylates p100 that can form a complex with RelB. The p100 subunit possesses an inhibitor function within the cytoplasm, and once phosphorylated it is ubiquitinated and partially degraded to produce the active subunit p52. The RelB and p52 heterodimer can then translocate to the nucleus and activate target transcription (Iwai, 2012) (see Figure 1.4).

The activation of the NF-κB pathway is tightly regulated by negative regulators like A20, CYLD and Cezanne. A20 knockout mice were unable to stop the TNF-α-induced activation of NF-κB. The importance of this was demonstrated by A20 knockout mice which showed a 100% mortality rate within 2 hours of an injection of the endotoxin lipopolysaccharide (LPS), an activator of the canonical pathway. 100% of the A20 heterozygous and homozygous wild type expressing mice survived 8 hours post the injection (Lee *et al.*, 2000). CYLD acts as a deubiquitinase (DUB) and removes K63 chains involved in IKK activation (Sun, 2010). Evidence also indicates that small non-coding ribonucleic acids (MicroRNAs) may also be involved in the downregulation of the NF-κB pathway (Zhou *et al.*, 2018).
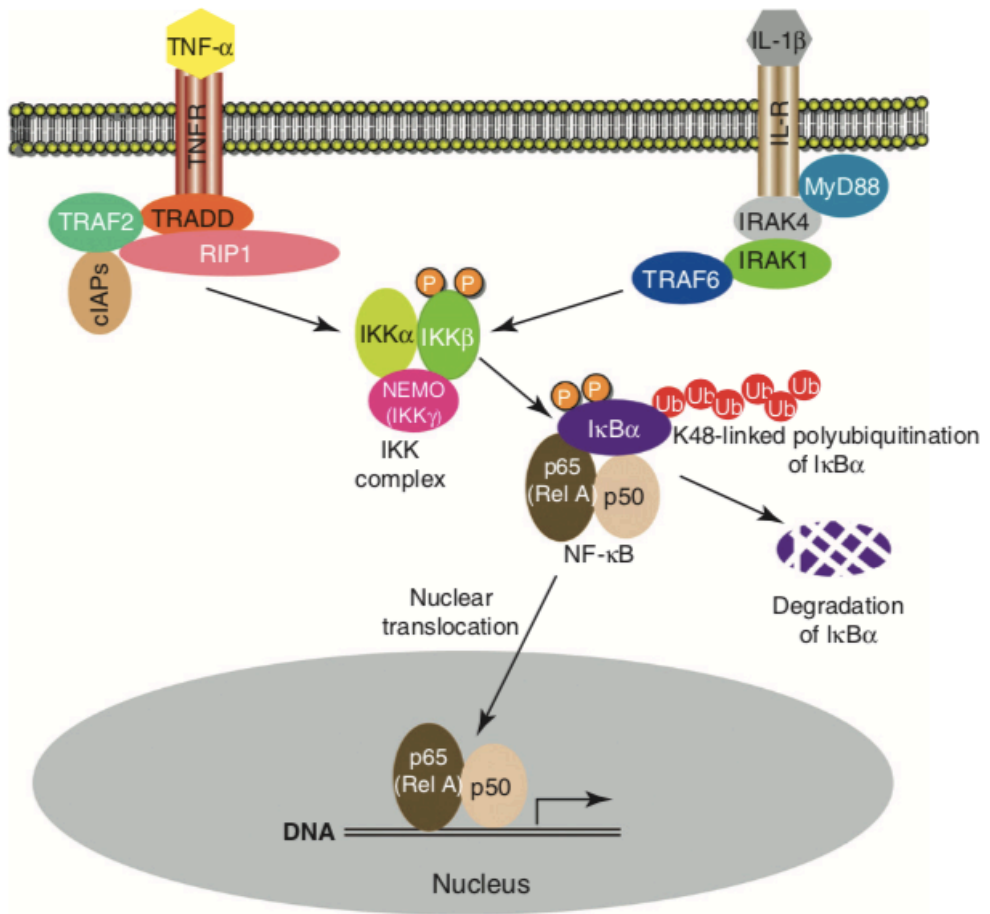
**Figure 1.3**

The canonical NF-κB pathway. Upon TNF-α binding to its receptor, IKKα is activated and phosphorylates the inhibitor IκBα, which is broken down in an ubiquitin-dependent manner. This releases the RelA/p50 heterodimer which can then translocate to the nucleus and activate transcription of target genes. Taken from (Iwai, 2012)
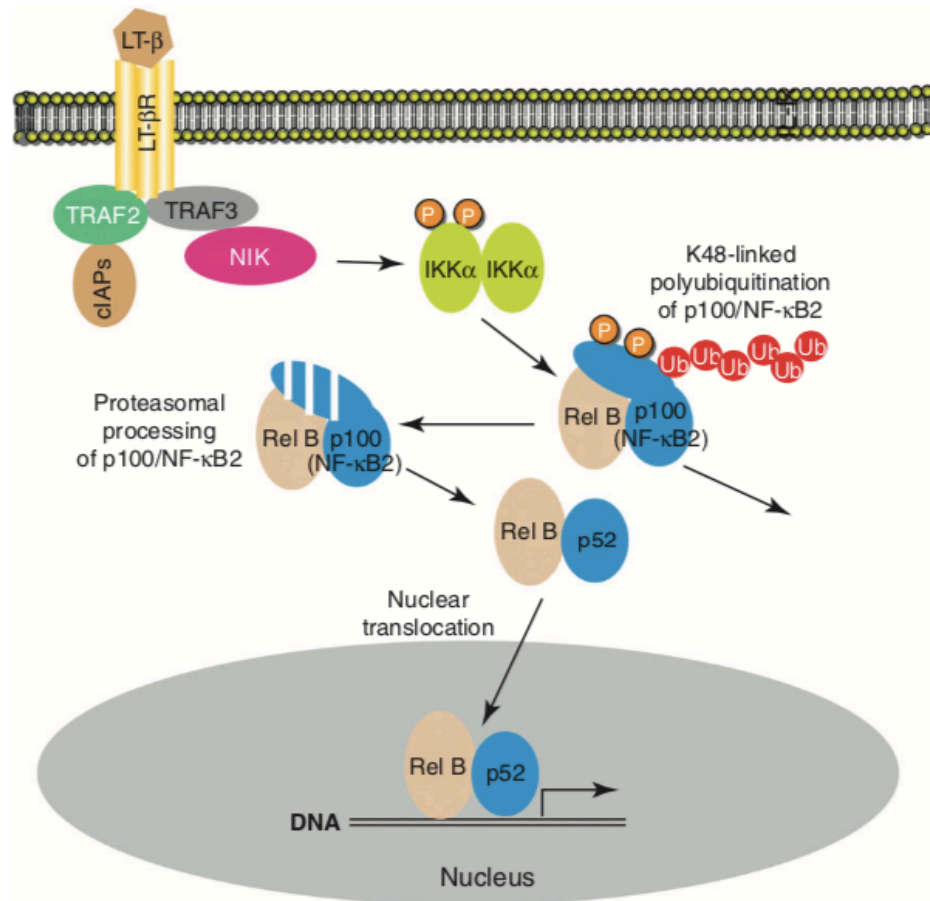
**Figure 1.4**

Non-canonical NF-κB pathway. When activators like lymphotoxin-β bind to their receptor, NIK is stabilised and phosphorylates IKKα. This triggers ubiquitin-mediated processing of p100 into p52, allowing the translocation of the RelB/p52 heterodimer to the nucleus. Here it binds to target DNA and activates transcription. Taken from (Iwai, 2012)

## 1.7 $CO_2$ and NF-κB

Although the use of lower tidal volumes is implemented to prevent further lung injury in ALI and ARDS patients, this still remains a controversial treatment option. While hypercapnia reduces inflammatory tissue damage, it appears to impair normal pathogenic responses and wound repair (Curley, Laffey and Kavanagh, 2010). One of the main pathways altered by hypercapnia is the NF-κB pathway, with responses to hypercapnia acidosis independent of mitosis, carbonic anhydrase, guanylyl cyclase, nitric oxide production, the hypoxia/oxygen sensing pathway, the heat shock pathway and the MAP kinases JNK, ER and P38 (O'Toole *et al.*, 2009; Cummins *et al.*, 2010; Wang *et al.*, 2010).

### 1.7.1 Canonical pathway and inflammatory signals

When $CO_2$ levels are increased from normocapnia to 10%, 15% and 20% $CO_2$ on HT-29 and the alveolar A549 cell lines, there is a significant dose dependent increase in the NF-κB inflammatory cytokines IL-6, IL-8 and monocyte chemoattractant 1 (MCP-1). Significant increases in nuclear translocation of p65 was also seen at 15% and 20% $CO_2$ but not at 10% (Abolhassani *et al.*, 2009). No alteration in p65 nuclear translocation was also seen in mouse embryonic fibroblasts (MEFs) when exposed to 10% $CO_2$ (Cummins *et al.*, 2010; Oliver *et al.*, 2012). Similarly, increasing $CO_2$ from ambient to 10% $CO_2$ levels in MEFs and primary human peripheral blood mononuclear cells (PBMC) showed a dose dependent increase in nuclear translocation of IKKα (seen in both the canonical and non-canonical pathway activation, see Figures 1.3 and 1.4) (Cummins *et al.*, 2010). However, this is technically a comparison between hypo- and hypercapnic conditions, and not between normo- and hypercapnic conditions. Despite this, all these data indicate that elevated $CO_2$ causes an increase in NF-κB induced inflammation. Interestingly, when A549 cells were stimulated with an inflammatory signal like TNF-α, hypercapnia reduced the TNF-α stimulated translocation of p65 to the nucleus, indicating that hypercapnia reduces inflammation if there is a background inflammatory signal. However, this study found no significant increase in p50/p65

heterodimer binding to DNA at 15% $CO_2$ (Masterson *et al.*, 2016), which would appear to contradict previous findings that elevated $CO_2$ does not alter translocation of p65. However, an elevation in p65 translocation to the nucleus does not indicate there is also an increase in p65 DNA binding.

TNF-$\alpha$-induced activation of NF-$\kappa$B in human bronchial epithelial and A549 cells was reduced by hypercapnia acidosis, as well as reduced TNF-$\alpha$ and endotoxin-induced secretion of IL-6 in small airway epithelial cells (SAEC) (Masterson *et al.*, 2016). Reductions in MCP-1 and TNF-$\alpha$ were also seen after hypercapnia treatment on TNF-$\alpha$ stimulated cells (Cummins *et al.*, 2010; Oliver *et al.*, 2012). However, this was in comparison to ambient $CO_2$ levels and not normocapnia conditions, meaning this finding has minimal physiological relevance.

Elevations in NF-$\kappa$B activation caused by the overexpression of IKK$\beta$ in A549 cells, were reduced after hypercapnia acidosis; and this effect was also seen after TNF-$\alpha$ stimulation within these cells. Hypercapnia acidosis appeared to inhibit the phospho-activation of IKK$\beta$, which reduced its ability to phosphorylate I$\kappa$B$\alpha$ (Masterson *et al.*, 2016). This would prevent the breakdown of I$\kappa$B$\alpha$ and therefore prevent the release of the NF-$\kappa$B subunits and the activation of the pathway.

Endotoxins like LPS are found on the outer layer of Gram-negative bacteria, stimulate the canonical pathway (Takeshita *et al.*, 2003) by binding to TLR4 (Wertz and Dixit, 2010). THP-1 macrophages, primary human, rat and mouse alveolar macrophages exposed to 20% $CO_2$, showed a significant reduction in LPS stimulated levels of TNF-$\alpha$ and IL-6 mRNA and protein (Lang *et al.*, 2005; Wang *et al.*, 2010). Prior incubation of cells for 1, 4 and 24 hours in hypercapnic conditions before LPS stimulation, did not alter the reduction in stimulation (Wang *et al.*, 2010). Hypercapnia attenuated the LPS-induced increase in NF-$\kappa$B DNA binding and IL-8 release within human pulmonary artery endothelial cells (HPAEC) (Takeshita *et al.*, 2003). Similarly, 10% $CO_2$ caused a significant reduction in LPS-stimulated increase in p65 translocation to the nucleus (Cummins *et al.*, 2010). Exposure of MEFs and HPAEC to 10% $CO_2$

significantly inhibited the LPS-induced degradation of IκBα (Takeshita *et al.*, 2003; Cummins *et al.*, 2010). However, a study using a higher concentration of $CO_2$ at 20% and the THP-1 macrophage cell line found no significant altering in LPS-induced IκBα degradation (Wang *et al.*, 2010). This would indicate that there could be a maximal effective dose for the effects of elevated $CO_2$. Not only this, but Wang *et al.* also used a 10 fold lower LPS dose which may also have influenced the result.

Transcriptome analysis of A549 cells stimulated with lymphotoxin-α1β2 and treated with 10% $CO_2$, highlighted transcriptional reductions in the pro-inflammatory molecules MCP-1, ICAM1 and TNF-α, but elevations in the anti-inflammatory IL-10 cytokine (Cummins *et al.*, 2010). RAW 264.7 cells transfected with an IL-6 promoter-driven luciferase reporter, demonstrated elevated $CO_2$ reduced LPS-stimulated IL-6 production and hypercapnia affected IL-6 transcription (Wang *et al.*, 2010). These studies would indicate that hypercapnia impacts on transcriptional levels of proteins within the NF-κB pathway.

Animal studies have shown beneficial effects of hypercapnia acidosis upon LPS stimulation. Both prior treatment with elevated $CO_2$ before LPS treatment and simultaneous treatment of elevated $CO_2$ and LPS, significantly reduced the bronchoalveolar lavage fluid (BALF) neutrophil count, indicating reduced inflammation. They also demonstrated that hypercapnia reduced lung injury after LPS treatment (Laffey *et al.*, 2003). This study however, did not look at anything specific to the effects of hypercapnia on the NF-κB pathway.

### 1.7.2 NF-κB, wound injury and pathogens

Hypercapnia acidosis blunted wound repair and NF-κB activation after wound injury in A549 cells. It reduced cellular migration and matrix metalloproteinase-1 but did not alter cellular mitosis (O'Toole *et al.*, 2009). Similarly, after ventilatory induced lung injury (VILI) hypercapnia reduced cellular repair and impaired membrane resealing within rats (Doerr *et al.*, 2005).

Despite this, hypercapnic acidosis reduced cytokine and wound injury activation of NF-κB in cells from rat systemic tissue and monocytes (Masterson *et al.*, 2016). Rat *in vivo* studies also found that after VILI, hypercapnic acidosis reduced nuclear levels of the canonical subunit p65 (indicative of reduced NF-κB activation) and reduced the cytokines TNF-α and MIP-2 within the BALF. Lung injury scores and neutrophil counts were also lower in the hypercapnic acidosis treated rats with VILI (Yang *et al.*, 2015). Cyclic stretch-induced injury on human bronchial epithelial (HBE and BEAS-2B) and alveolar A549 cells increased IL-8 release which was attenuated when treated with hypercapnic acidosis. This strong attenuation in IL-8 release was seen over a five-day period within the A549 cells. Similarly, hypercapnic acidosis also abolished cyclic stretch-induced cell membrane injury and progressive cell death in A549 cells. Interestingly, preconditioning cells to elevated $CO_2$ was less effective than post-conditioning for reducing cyclic stretch injury-induced IL-8 release (Horie *et al.*, 2016).

Rats with pneumonia-induced acute lung injury which overexpressed the NF-κB inhibitor, IκBα, or treated with hypercapnic acidosis showed significant reduction in NF-κB activation (Devaney *et al.*, 2013; Masterson *et al.*, 2016). If injury to rat lungs or A549 cells occurred when IκBα was overexpressed and subsequent treatment of hypercapnic acidosis was given, no further increase in the reduction of NF-κB activation was seen (Horie *et al.*, 2016; Masterson *et al.*, 2016). Post *Escherichia coli* induced injury, both hypercapnic acidosis and IκBα overexpression improved the 50% survival rate seen in the normocapnic treatment group, with IκBα overexpression alone or with hypercapnic acidosis conferring a 100% survival rate (Masterson *et al.*, 2016). Contrary to this, 100% of mice exposed to 3 days of 10% $CO_2$ prior *Pseudomonas aeruginosa* infection died after 48 hours compared to air exposed mice, which had a 50% and 30% survival rate after 48 and 96 hours respectively (Gates *et al.*, 2013). Interestingly, in the hypercapnic acidosis group the BALF cytokine levels of IL-6 and TNF-α were significantly reduced after 7 but not 15 hours following *P. aeruginosa* infection (Gates *et al.*, 2013). These two studies are

looking at two different types of bacteria, and therefore this could mean that hypercapnia has a different effect on the *E. coli* infections vs *P. aeruginosa* infections.

In prolonged pneumonia-induced acute lung injury, IκBα overexpression increased lung *E. coli* bacterial load and histological lung injury within rats (Devaney *et al.*, 2013). Not only this, but hypercapnia also reduced human macrophage ability to kill bacteria like *P. aeruginosa* (Casalino-Matsuda *et al.*, 2015) and to phagocytose heat killed *Staphylococcus aureus* (Wang *et al.*, 2010). Exposure of mice to 10% $CO_2$ caused both a reduction in phagocytosis function and hydrogen peroxide ($H_2O_2$) production (found within lysosomes and involved in breaking down phagocytosed material), and after 15 hours of infection there was a fourfold increase in *P. aeruginosa* compared to air exposed mice. Any increases in bacterial load were not due to hypercapnia affecting *P. aeruginosa* growth, as *in vitro* growth was slowed in bacteria grown in elevated $CO_2$ conditions (Gates *et al.*, 2013). Of note the efficacy of the beta-lactam antibiotic ceftriaxone, appeared to be unaffected by hypercapnic conditions *in vivo* in rats against an *E. coli* infection (O'Croinin *et al.*, 2008).

Although studies agree hypercapnia acidosis reduces injury-induce NF-κB activity, there is not complete agreement whether hypercapnia acidosis improves or reduces wound injury and overall survival.

### 1.7.3 The non-canonical pathway

Evidence indicates that hypercapnia affects the non-canonical pathway as well as the canonical pathway. Elevated $CO_2$ levels on MEFs results in a rapid, dose dependent and reversible cleavage and nuclear translocation of RelB (Oliver *et al.*, 2012; Keogh *et al.*, 2017). Not only this, elevated $CO_2$ levels caused a dose dependent increase in p100 translocation to the nucleus in both MEFs and A549 cell lines (Keogh *et al.*, 2017). Stimulation of MEFs and A549 cell lines with LPS under elevated $CO_2$ conditions, resulted in an enhanced RelB cleavage and nuclear localisation. Hypercapnia treatment *in vivo* with LPS intratracheal installation, resulted in a significant increase in leukocyte nuclear RelB staining compared to control

conditions. This was also associated with an improved survival, lung function and significant degree of lung protection against inflammation (Oliver *et al.*, 2012). RelB protein-protein interactions appear to be altered by hypercapnic conditions. Residues 483-504 of the C-terminus which contains the transactivation domain of RelB, appears to be processed in a $CO_2$ dependent manner (Keogh *et al.*, 2017).

## 1.8 Effects of pH on the NF-κB pathway

As previously discussed, when $CO_2$ levels are elevated there are increases in $H^+$ concentrations (see figure 1.1), causing a reduction in overall pH. Therefore, the alterations to the NF-κB pathway caused by hypercapnia could be caused by changes in $CO_2$, pH or a combination of both.

When the pH of the media was reduced from 7.5 to 5.0 on rabbit alveolar macrophages, there was a significant reduction in LPS stimulated TNF-α production (Bidani *et al.*, 1998). However, this acidosis is far greater than the pH changes seen under hypercapnic conditions, and not physiologically relevant. Despite this, similar results were found when media pH was dropped from 7.4 to 7.0 on the murine J774 macrophages, with significant reductions in both TNF-α and IL-6 after LPS stimulation. However, in the human THP-1 and human monocyte derived macrophage cell lines, reducing the pH to 7.0 showed no significant alteration in LPS stimulated TNF-α production (Gerry and Leake, 2014). Similarly, after TNF-α stimulation and reduced pH treatment on human gastric epithelial cells, no alteration in NF-κB translocation was seen (O'Toole *et al.*, 2005). After TNF-α stimulation, THP-1 cells also showed no alteration in nuclear localisation of the p50:p105 heterodimer or level of p50:p50 and p50:p65 dimers binding to DNA; but J774 cells did (Gerry and Leake, 2014). Similarly, the level of IL-8 secretion was not significantly altered across media pH 6.5, 6.7, 6.9 or 7.28 on HT-29 or A549 cells over a 48 hour period (Abolhassani *et al.*, 2009), potentially indicating that reductions in pH do not affect human cells.

No difference in TNF-$\alpha$ secretion was seen between J774 macrophages when the pH was dropped from 7.4 to 7.0 (Gerry and Leake, 2014). However, when media pH is reduced from 7.4 to 6.6 on human gastric epithelial cells, NF-$\kappa$B DNA binding is enhanced from 30 minutes up to 24 hours. In fact, when pH levels were elevated above 7.8 the NF-$\kappa$B DNA binding fell. Similarly, when low pH and *Helicobacter pylori* are given together on human gastric epithelial cells, there are elevated increases to *H. pylori* induced NF-$\kappa$B nuclear translocation and degradation of I$\kappa$B$\alpha$ (O'Toole *et al.*, 2005). However, once again this acidosis is far greater than that seen with hypercapnia acidosis.

When the pH was controlled under hypercapnic conditions in MEFs, the level of suppression seen in LPS-induced p65 nuclear accumulation and I$\kappa$B$\alpha$ cytoplasmic degradation was the same compared to hypercapnic acidosis conditions. There was also no significant difference found in the intracellular pH of MEFs exposed to 10% $CO_2$ (Cummins *et al.*, 2010). Controlling the pH on THP-1 cells exposed to 12.5% $CO_2$ did not alter the reduction in IL-6 after LPS stimulation. Reducing the pH from 7.2 to 6.5 on THP-1 cells caused progressive attenuations in LPS-induced increase in IL-6. However, this reduction would have been a 500% increase in $H^+$, compared to a 60% increase in $H^+$ seen with the hypercapnia reduction in pH from 7.2 to 7.0. This indicates that the pH and hypercapnic reductions seen here occur via different mechanisms (Wang *et al.*, 2010). Similar findings have been found for the non-canonical pathway. Reducing media pH to 6.8 on MEFs had no effect on RelB translocation to the nucleus; whereas physiological pH and 10% $CO_2$ resulted in RelB cleavage and nuclear localisation (Oliver *et al.*, 2012).

Despite all this evidence pointing to the elevated $CO_2$ causing the effects seen by hypercapnia acidosis, there is also evidence which indicates it could be the pH. Both low pH with physiological $CO_2$ levels and physiological pH with elevated $CO_2$ on HPAECs inhibited LPS-induced NF-$\kappa$B DNA binding and I$\kappa$B$\alpha$ degradation. Although these were to a lesser degree than hypercapnia acidosis (reduced pH and elevated $CO_2$) (Takeshita *et al.*, 2003). After cell stretch-induced injury to HBE, BEAS-2B and

A549 cell lines hypercapnia acidosis significantly inhibited IL-8 secretion, increased cellular survival and reduced membrane injury. When the pH was buffered at 15% $CO_2$ no significant improvement in cell survival, reduction in IL-8 release or reduced induction of NF-κB was seen by A549 cells. Similarly, metabolic acidosis without an increase in $CO_2$ significantly improved cell survival, and reduced IL-8 release and induction of NF-κB (Horie et al., 2016).

In vivo studies do not always control for alterations in arterial blood pH, and when $CO_2$ levels are elevated the pH significantly drop compared to normocapnic treatments (Doerr et al., 2005; Contreras et al., 2012; Yang et al., 2015). Higher $CO_2$ levels causes a larger pH drop (Abolhassani et al., 2009; Yang et al., 2015). After only 1 hour for rats and 2 hours for mice exposed to 10% $CO_2$, arterial blood pH significantly dropped from normocapnic levels (Gates et al., 2013; Yang et al., 2015). They remained at this level for the full 4 hours of the study period (Yang et al., 2015). However, a significant difference in pH was not found in rats inhaling 5% $CO_2$ and given an intratracheal installation of LPS (Laffey et al., 2003). If mice exposed to 10% $CO_2$ for 3 days, renal compensation for the acidosis caused by the hypercapnia occurred. No difference was seen between inoculation with P. aeruginosa prior and post renal compensation for acidosis, indicating the reduced survival was not caused by acidosis but hypercapnia (Gates et al., 2013). In another study which produced buffered hypercapnia subjects, exposed rats to 8% $CO_2$ for 4 days to allow renal compensation. When this group was directly compared to rats with hypercapnic acidosis, and only the hypercapnic acidosis group showed a reduction in systemic sepsis induced lung injury (Higgins et al., 2009).

Overall, the overlapping and conflicting conclusions from these studies make it difficult to conclusively demonstrate that the overall effect of hypercapnia is caused by $CO_2$ alone, pH or a combination of both.

### 1.8.1 Why are there different findings between studies?

The evidence on the effect of hypercapnia on the NF-κB pathway appears to be highly conflicting, with evidence indicating the secondary reductions in pH, just elevations in $CO_2$ and even both together are the primary effectors of hypercapnia acidosis on the NF-κB pathway. The effects also range from $CO_2$ alone causing elevations in NF-κB activation to hypercapnia reducing NF-κB activation in models with background inflammation.

There are many factors which could affect the findings across these different studies. These include: cell line, level of elevated $CO_2$, stimulus of the pathway, NF-κB activation measurement output, time course for assays, level of pH buffering, *in vivo* vs *in vitro* and animal model used. All of these may influence the outcome of the study and may explain why the overall effect of hypercapnia is so confusing. For instance, although LPS and TNF-α both stimulate the canonical NF-κB pathway and ultimately activate NEMO and IKKα, the signalling prior to this point is different. LPS binds the receptor TLR4 and TNF-α binds to TNFR1, and LPS activates the adaptors TRAM or MAL, while TNF-α activates the adaptor TRADD (see Figure 1.4 for further details). Not only this but LPS is a stimulant of both the canonical and non-canonical pathway, which could complicate the output signal. Therefore, any differences seen between the effects of hypercapnia across LPS and TNF-α, may be caused by alterations to different molecules along the pathway or through the production of a messy signal produced by the LPS. A summary table has been made to help clarify the findings across studies mentioned here (see Table 1.1).
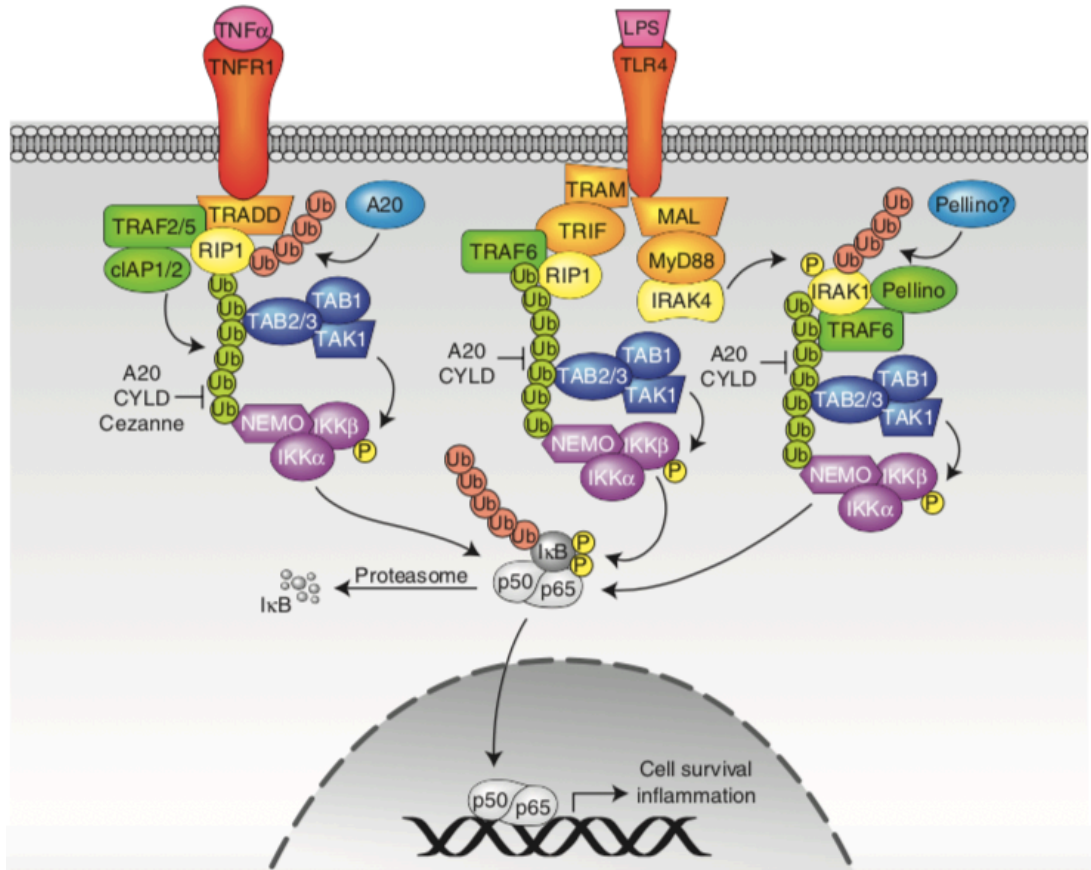
**Figure 1.5**
Canonical pathway activation by LPS and TNF-α. Although they activate different receptors they both lead to the activation of the IKK complex consisting of NEMO, IKKα and IKKβ; which leads to the breakdown of the IκBα, releasing the NF-κB subunits. Taken from (Wertz and Dixit, 2010)

## 1.9 Ubiquitin

Ubiquitin PTM's are essential for the activation of both the canonical and alternative NF-κB pathways (see Figure 1.3 and 1.4). Ubiquitin is a highly conserved globular protein of 76 amino acids and covalently attaches to target substrates (Skaug, Jiang and Chen, 2009). It can tag proteins as a monomer or polymers and the formation of polyubiquitin chains are formed by linking via one of the 7 lysine residues (K6, K11, K27, K29, K33, K48 and K63) or via the N-terminal methionine. Polyubiquitin chains

can be homotypic or heterotypic in terms of lysine linkage, with different polyubiquitin chain formations possessing different signals (Iwai, 2014). For instance, K48-linked polyubiquitin signals for protein degradation via the 26S proteasomal pathway (Chau *et al.*, 1989; Akutsu, Dikic and Bremm, 2016), while K63 linked chains are involved in DNA repair (Spence *et al.*, 2015). Ubiquitin binding domains (UBDs) recognise the different polyubiquitin chains, through the hydrophobic region around residues 136 and 144. The relative positioning of these two residues is characteristic across the polyubiquitin chains (Akutsu, Dikic and Bremm, 2016).

The ubiquitin-proteasome system is crucial for NF-$\kappa$B activation, making K48 polyubiquitin chains of particular interest. There are 3 major enzymes each with many variants within the ubiquitin-proteasome system; E1, E2 and E3. Using ATP E1, an ubiquitin-activating enzyme, forms a thiol-ester bond between itself and ubiquitin. The activated ubiquitin is then transferred to E2, an ubiquitin-conjugating enzyme. The ubiquitin is then transferred across to the HECT or RING domain found on E3, an ubiquitin-ligating enzyme, before forming an isopeptide bond with the $\epsilon$-amino group of a lysine residue within the target substrate and ubiquitin (Skaug, Jiang and Chen, 2009). It is the HECT containing E3 enzymes or RING containing E2 enzymes that determine the ubiquitin linkage specificity (Wertz and Dixit, 2010).

### 1.9.1 Ubiquitin and NF-$\kappa$B pathway activation

One of the most important polyubiquitin chains involved in NF-$\kappa$B activation are K48 polyubiquitin chain. K48 polyubiquitination occurs on I$\kappa$B$\alpha$, signalling for its degradation and releases the NF-$\kappa$B subunits.

Development of ubiquitin chain linkage specific antibodies demonstrated K63 associated with RIP1 within 5 minutes of TNF-$\alpha$ stimulation. But after 10 minutes, K48 chains were detected before this signal diminished at later time points, presumably due to proteasomal degradation (Newton *et al.*, 2008).

K63 and Methionine-linked (M1) polyubiquitin chains are involved in the activation of the IKK complex within the canonical pathway. M1 chains are assembled by the E3 enzyme LUBA, and are attached to NEMO, a subunit within the IKK complex. NEMO contains a M1-chain-specific UBD required for full IKK activation (Tokunaga *et al.*, 2009). M1-K63 hybrid chains also activate the IKK complex in response to IL-1 and TLR 1/2 ligands. K63 chains are attached to the IL-1 receptor, before M1 modifications are subsequently added. K63 chains bind to TAK1 components while the M1 chains bind to the NEMO M1-specific UBD, allowing the activation of the IKK$\alpha$ and IKK$\beta$ subunits of the IKK complex (Emmerich *et al.*, 2013).

There is evidence that K11 chains are also involved in the canonical pathway. K11 chains associated with the TNFR1-bound RIP1 after TNF-$\alpha$ stimulation. After TNF-$\alpha$ stimulation the UBD of NEMO can bind to K11, K48, K63 and M1 ubiquitin chains (Dynek *et al.*, 2010).

Another method of NF-$\kappa$B regulation is ubiquitin editing, in which DUBs and ubiquitin ligases alter the ubiquitin status of key proteins within the NF-$\kappa$B pathway. Ubiquitin editing attenuated NF-$\kappa$B activity in the canonical pathway but promoted activity in the alternative pathway. DUBs deubiquitylate K63 chains, disassemble platform signalling molecules before K48 chains are polymerised onto the same target protein for proteasomal degradation (Wertz and Dixit, 2010).

## 1.10 Hypothesis

We hypothesise that K48 of ubiquitin becomes carbamylated during conditions of elevated $CO_2$. The would then prevent polyubiquitin formation and prevent the degradation of IκBα, inhibiting activation of the NF-κB pathway under these conditions.

Cells which were re-equilibrated to ambient conditions lost the effect of hypercapnia on IL-8 release and IKK nuclear accumulation (Cummins *et al.*, 2010; Wang *et al.*, 2010). This reversible effect was also seen in *in vivo* models, with mortality rates after *P. aeruginosa* infection improving by 20% if mice were removed from hypercapnic to ambient conditions (Gates *et al.*, 2013). The rapid reversal of the hypercapnic effects indicates the mediator for the effects of elevated $CO_2$ is a PTM. Not only this but lysine residues are a known target for carbamylation; both factor support our hypothesis.

K48 linked polyubiquitin chains are important for signalling proteasomal degradation of the canonical inhibitor, IκBα. Hypercapnic acidosis has shown to reduce TNF-α induced degradation of IκBα, but not cause an increase in IκBα production or reduce TNF-α-induced gene transcription of IκBα (Masterson *et al.*, 2016). All of which indicate that the turnover of IκBα is being altered by hypercapnic acidosis. If the carbamylated K48 residue is unable to form as polyubiquitin chain, it would prevent the degradation signal for IκBα and inhibit activation of the NF-κB pathway under elevated $CO_2$ conditions.

**Table 1.1** Summary table of literature discussed in the introduction

| Cell Line | In vivo | Stimulus | CO$_2$ % | CO$_2$ | pH | pH not controlled | Response | Reference |
|---|---|---|---|---|---|---|---|---|
| A549 | - | lymphotoxin -α1β2 | 10% | | | X | Reduced CCL2 and ICAM-1, increased IL-10 | Cummins et al., 2010 |
| | - | N/A | 10% | X | | | Increased nuclear localisation and cleavage of RelB, increased nuclear translocation p100 | Keogh et al., 2017 |
| | - | N/A | 10% | X | | | Increased RelB nuclear translocation, IKKα rapid nuclear accumulation. (Reduced TNF-α stimulated TNF-α release) | Oliver et al., 2012 |
| | - | N/A | 10-20% | X | | | Increased IL-6, IL-8 and MCP-1, increased p65 translocation only at 15% and 20% CO$_2$ (found an involvement of protein phosphatase 2) | Abolhassani et al., 2009 |
| | - | Wound | 10% & 15% | X | | | Reduced wound closure, reduced cellular migration with and without injury | O'Toole et al., 2009 |
| | - | Cell stretch | 10% & 15% | | | X | Inhibited NF-κB activation, reduced IL-8 production, reduced cell injury and lysis, increased cell viability | Contreras et al., 2012 |
| | - | Cyclic stretch injury | 15% | | X | | Inhibited NF-κB activation, reduced IL-8 secretion, reduced membrane injury, increased cell survival, inhibited degradation of IκBα | Horie et al., 2016 |
| | - | TNF-α | 15% | | | X | Reduced NF-κB activation, reduced IKKβ-overexpression activation of NF-κB with and without TNF-α, reduced NF-κB bound to consensus sequence on DNA, inhibited p65 nuclear translocation | Masterson et al., 2016 |
| | - | Wound | 15% | | | X | Blunted repair, reduced NF-κB activation, reduced cellular migration | Masterson et al., 2016 |
| SAEC | - | Wound | 15% | | | X | Reduced wound closure | O'Toole et al., 2009 |

| Cell type | | Stimulus | % | | | | Effect | Reference |
|---|---|---|---|---|---|---|---|---|
| | - | TNF-α and LPS | 15% | | | X | Reduced IL-8 secretion | Masterson et al., 2016 |
| | - | Wound | 15% | | | X | Blunted repair, reduced NF-κB activation | Masterson et al., 2016 |
| **Human bronchial epithelial cells** | - | Cyclic stretch injury | 15% | | | X | Reduced membrane injury and rupture, reduced cell death | Horie et al., 2016 |
| | - | TNF-α | 15% | | | X | Reduced NF-κB activation, reduced IκBα degradation, reduced TNF-α induced increase in IκBα transcription | Masterson et al., 2016 |
| | - | Wound | 15% | | | X | Reduced wound closure | O'Toole et al., 2009 |
| **HPAEC** | - | LPS | 10% | X | X | | Reduced NF-κB DNA binding, inhibited degradation in IκBα, inhibited ICAM-1 and IL-8 mRNA production, LDH release reduced | Takeshita et al., 2003 |
| **PBMC** | - | TNF-α | 10% | | | X | Increased IKKα nuclear translocation | Cummins et al., 2010 |
| **Human alveolar macrophages** | - | LPS | 20% | | | X | Reduced TNF-α and IL-6 synthesis, inhibited phagocytosis of opsonised polystyrene beads | Wang et al., 2010 |
| **Rabbit alveolar macrophages** | - | LPS | N/A | | X | | pH reduced from 7.4 - 5 reduced TNF-α release | Bidani et al., 1998 |
| **THP-1** | - | LPS | 15% | X | | | Inhibited autophagy (also inhibited autophagy induced by *S. aureus* and *E. coli*) | Casalino-Matsuda et al., 2015 |
| | - | LPS | 20% | X | X | | Reduced IL-6 and TNF-α mRNA and protein, reduced uptake of heat-killed *S. aureus* and phagocytosis, dropping pH to 6.5 reduced IL-6 release. Likely pH and $CO_2$ were affecting via different mechanisms | Wang et al., 2010 |
| | - | LPS | N/A | | X | | pH 7.0: no effect on TNF-α secretion | Gerry and Leake, 2014 |

36

| | | | | | | | |
|---|---|---|---|---|---|---|---|
| | - | TNF-α | N/A | | X | pH 7.0: no effect on p50/p105 nuclearisation, no effect p65:p50 or p50:p50 DNA-binding | Gerry and Leake, 2014 |
| HEK 293 | - | N/A | 10% | X | | RelB cleaved at C terminus | Keogh et al., 2017 |
| HT-29 | - | N/A | 10-20% | X | | Increased IL-6 and MCP-1, increased p65 translocation only at 15% and 20% $CO_2$ (found an involvement of protein phosphatase 2) | Abolhassani et al., 2010 |
| MEFs | - | LPS | 10% | X | | RelB cleaved and translocated to nucleus (both with and without LPS stimulation), IKKα rapid nuclear accumulation | Oliver et al., 2012 |
| | - | LPS | 10% | X | | Significantly reduced NF-κB activity, increased IKKα nuclear translocation, inhibited nuclear p65, reduced CCL2 induction | Cummins et al., 2010 |
| | - | N/A | 10% | X | | Increased nuclear localisation and cleavage of RelB, increased nuclear translocation p100 | Keogh et al., 2017 |
| Mouse macrophages | - | LPS | N/A | | X | pH 7.0: reduced TNF-α secretion, IκBα remained low, increased IκBα mRNA, | Gerry and Leake, 2014 |
| | - | TNF-α | N/A | | X | pH 7.0: increased nuclear p50/p105, increased p65:p50 and p50:p50 DNA-binding | Gerry and Leake, 2014 |
| Mouse alveolar macrophages | - | LPS | 20% | | X | Reduced TNF-α and IL-6 synthesis | Wang et al., 2010 |
| RAW 264.7 | - | LPS | 20% | | X | Reduced IL-6 mRNA expression | Wang et al., 2010 |
| Primary Type II Rat Alveolar Epithelial Cells | - | Wound | 15% | | X | Impaired membrane resealing, increased permanent cell damage | Doerr et al., 2005 |
| Rat Alveolar Macrophages | - | LPS | 10% & 20% | X | | Dose dependent reduction in TNF-α release | Lang et al., 2005 |

| | | Model | % | | | | Findings | Reference |
|---|---|---|---|---|---|---|---|---|
| - | **Mice** | N/A | 5-15% | | | X | Increased RANTES, MIP-1α, MIP-1β and MCP-1 RNA, increased transcription TCA-3, eotaxin and IP-10 | Abolhassani et al., 2010 |
| - | | *Pseudomonas aeruginosa* pneumonia | 10% | X | | | Increased mortality rates, increased bacterial load in lungs, spleen and liver, no difference in lung injury compared to normocapnia, impaired neutrophil function, reduced IL-6 and TNF-α 7 hours after infection | Gates et al., 2013 |
| - | **Rats** | Severe VILI | 5% | | | X | Increased survival, reduced lung injury, increased $O_2$ partial pressure, increased static lung compliance, reduced neutrophil counts, reduced IL-6, TNF-α and CINC-1, reduced histological injury | Contreras et al., 2012 |
| - | | LPS | 5% | | | X | Increased static lung compliance and pulmonary inflammation | Laffey et al., 2004 |
| - | | VILI | 12% | | | X | Inhibited wound repair | Doerr et al., 2005 |
| - | | VILI | 11-17% | | | X | Reduced neutrophil counts, reduced TNF-α and MIP-2 in BALF, reduced lung injury score, reduced ICAM-1 expression, reduced NF-κB activity, reduced p65 nuclear translocation, inhibited reduction in IκBα | Yang et al., 2015 |
| - | | *Escherichia coli* pneumonia | N/A | - | - | - | IκBα overexpression: increased survival, reduced histological injury. Effects lost with prolonged pneumonia. | Devaney et al., 2013 |

# 2 - Materials and Methods

## 2.1 Materials

All materials were purchased from Merck (formerly Sigma-Aldrich) unless stated otherwise.

## 2.2 Cell lines

The human embryonic kidney (HEK 293) reporter cell line NF-$\kappa$B/293/GFP-Luc$^{TM}$ was used for all assays unless stated otherwise and was purchased from Systems Biosciences. Also used was the human glioma reporter cell line U251-NF-$\kappa$B-GFP-Luc which was provided by Dr Darius Widera (University of Reading). Both reporter cell lines were used to quantify NF-$\kappa$B activity.

## 2.3 DNA Plasmids

All DNA plasmids were purchased from Addgene.

## 2.4 Routine Mammalian Cell Culture

All mammalian cell culture was carried out in a Class II biosafety cabinet to minimise infection of cultures. To further prevent infection equipment not already sterilised was autoclaved and all equipment moved into the hood was sprayed with 70% (v/v) ethanol.

### 2.4.1 Passaging of cell

Cells were grown at 37 °C in 5% $CO_2$, 21% $O_2$ and humidified conditions. The NF-κB/293/GFP-Luc$^{TM}$ cells were maintained in complete growth media made up of 89% (v/v) Dulbecco's Modified Eagle Medium (DMEM) (Fisher Scientific UK), 10% (v/v) heat inactivated Fetal Bovine Serum (FBS) and 1% (v/v) Penicillin-Streptomycin antibiotic (PenStrep). The U251-NF-κB-GFP-Luc cell line was grown in complete growth medium but without PenStrep. Cultures were monitored via light microscopy and passaged at a confluency no greater than 90% to maintain a healthy culture and prevent cell death. When passaging cells the old media was aspirated and cells were washed with sterilised 1x PBS prewarmed to 37 °C to remove any residual media. To remove the adhered cells from the flask cells were then treated with 0.1% (w/v) Typsin-EDTA solution and incubated for 5-10 minutes at 37 °C in the 5% $CO_2$ incubator. Trypsin was then neutralised by adding complete growth media preheated to 37 °C. Cells were then split into a fresh sterile flask, or when carrying out an assay cells were seeded onto 24 well plates. Plates and culture flasks were obtained from Fisher Scientific UK.

### 2.4.2 Cell storage and retrieval

Cells were cryopreserved at -150 °C in complete growth media supplemented with 10% dimethyl sulfoxide (DMSO). Upon retrieval cells were immediately placed into a water bath at 37 °C and gently agitated for 1 minute and 30 seconds. Cells were added to complete growth medium preheated to 37 °C and centrifuged for 5 minutes at room temperature at 200 x*g*. Once centrifuged, the media containing DMSO was

discarded and cells resuspended in complete growth medium preheated to 37 °C and placed into a sterile flask. The cells were then maintained in a 37 °C incubator with 5% $CO_2$, and the media was replaced every 48 hours to prevent nutrient depletion.

### 2.4.3 Freezing cells

Cells were passaged according to 2.4.1, but cells were placed into a falcon tube rather than a fresh flask and centrifuged for 10 minutes at 250 x*g* at room temperature. Media was then aspirated and the cells resuspended in chilled complete growth medium supplemented with 10% (v/v) DMSO. The suspension of cells were then placed into cryovials and frozen at -80 overnight, before being frozen and stored at -150 °C.

## 2.5 Molecular Biology

### 2.5.1 Bradford assay

5 μl of known protein concentrations of Bovine Serum Albumin (BSA) (0-1 mg/ml) diluted in 1x PBS was mixed with 150 μl of Bradford Reagent. The absorbance at 595 nm was measured and protein concentration was plotted against absorbance for the standard curve. A standard curve was created per assay. To estimate sample lysate protein concentration, 5 μl of sample was mixed with 150 μl of Bradford reagent before reading the absorbance. The protein concentration was estimated from the standard curve. 3 technical replicates were carried out per sample and an average absorbance calculated. The cell count was not calculated in assays as this would have been too time consuming for the high quantity of samples used in each experiment, and the Bradford assay allowed a higher throughput. It was therefore assumed that protein concentration was proportional to the cell count.

### 2.5.2 Luminescence and Fluorescence readings

20 μl of lysate was mixed with 50 μl of the Luciferase substrate, both equilibrated to room temperature, and the luminescence signal (Luc) was read immediately for 5 minutes every 16 seconds. 50 μl of lysate was used to measure the fluorescence signal (485/530 nm). Both were measured on the Synergy$^{TM}$ H4 Hybrid Multi-Mode Microplate Reader. The Luc and fluorescent signals were normalised to μg of protein estimated from a Bradford assay.

## 2.6 NF-κB activity assays

### 2.6.1 Assay media

For all assays unless stated otherwise, cells were seeded onto 24 well plates in complete growth medium and grown to 60-80% confluency at 5% $CO_2$. Confluency was determined by light microscopy. At the start of an assay complete growth medium was aspirated and replaced with assay media (see Table 2.1) which had been incubated at either 5% or 10% $CO_2$ for 6 hours. The complete growth medium contained a set amount of bicarbonate (3.7 mg/L) and resulted in different end pH values for the 5% and 10% $CO_2$ samples (data not shown), hence it was replaced with media which allowed the bicarbonate levels to be altered. Samples of the assay media had the pH measured before being placed on cells, and then samples of assay media at the end of the assay was also measured using a AB150 benchtop pH meter (Fisher Scientific UK).

**Table 2.1**
Sodium bicarbonate levels were added to DMEM used in assays. 'Original Media' was based on Oliver et al. 2012. 'Assay Media' was sodium bicarbonate levels required to achieve the same media pH at the end of an assay at both 5% and 10% $CO_2$. The DMEM contained 10% (v/v) FBS and 1% (v/v) PenStrep but no phenol red. In assays carried out on the U251-NF-κB-GFP-Luc cell line the PenStrep was omitted from the media as specified by the cell line protocol.

|  | Ambient $CO_2$ levels | 5% $CO_2$ levels | 10% $CO_2$ levels |
|---|---|---|---|
| **Original Media** | 0.96 g/litre | 2.46 g/litre | 4.42 g/ml |
| **Assay Media** | - | 3.8 g/litre | 4.4 g/litre |

### 2.6.2 Dose response assays

The complete growth media was replaced with original/assay media and TNF-α doses ranging from 0.1-30 ng/ml were added. TNF-α was diluted in sterilised 1x PBS solution pre-warmed to 37 °C, and 1x PBS was added to control samples. Cells were

then placed in the 5% or 10% $CO_2$ incubator. After 2, 6 or 18 hours, media was aspirated and 100 $\mu$l of ice cold 1x PBS/well was added to resuspend cells. To lyse cells and release the cellular protein, samples were sonicated for 4 seconds and then immediately placed on ice. Luc and fluorescence was then measured and normalised to $\mu$g of protein, determined by a Bradford assay.

### 2.6.3 DNA plasmids

Previously in the lab, glycerol stocks were made of DH5$\alpha$ cells transduced with DNA containing the pRK5 vector, pRK5-HA-Ubiquitin-K48R and pRK5-HA-Ubiquitin-K63R plasmids obtained from Addgene. Overnight cultures were obtained from these stocks.

### 2.6.4 Miraprep

The Miraprep protocol is an adaption of the Spin Miniprep Kit (QIAGEN) protocol used for DNA purification and amplification (Pronobis, Deuitch and Peifer, 2016). An overnight culture of 50 mL of Luria Broth (LB) was centrifuged at 4,200 x$g$  for 5 minutes. The supernatant was removed, and the pellet was resuspended in 2 mL of resuspension buffer. 2 mL of lysis solution was mixed with the pellet by inverting the tube 3-4 times, before 2 mL of neutralisation solution was added and the tube inverted 3-4 times. The solution was then split across 1.5 mL Eppendorf tubes, and spun for 10 minutes at 13,200 x$g$. The supernatant was then collected into a single 15 mL falcon tube and 5 mL of 96% (v/v) ethanol was mixed with the solution. This solution was then loaded onto spin columns and centrifuged for 30 seconds at 13,200 x$g$. 500 $\mu$l of wash solution was added to the column, centrifuged for 30 seconds at 13,200 x$g$ and the flow through was discarded. The column was then transferred to a fresh Eppendorf and 35 $\mu$l of deionised $H_2O$ was added to the column and incubated at room temperature for 1 hour. The DNA was collected by centrifuging the column for 2 minutes at 13,200 x$g$. DNA quantification was determined by using a Nanodrop (ThermoFisher). The DNA was then stored at -20 °C.

### 2.6.5 Transfection assays

Transfection of the pRK5 vector and pRK5 vector containing K48R or K63R mutant ubiquitin DNA into cells was carried out using the Invitrogen™ Lipofectamine™ 3000 Transfection Reagent (Fisher Scientific UK) according the manufacturer's instructions. Cells were grown to ~60% confluency at the time of transfection. The transfection efficiency was measured by transfecting the green fluorescent protein (GFP) into cells and visualising protein translation by fluorescence microscopy and measuring the fluorescence signal on a plate reader from the cell lysate. Cells were transfected for 20 hours before treatment with TNF-$\alpha$ for 18 hours. Assay media was added just before TNF-$\alpha$ treatment and immediately placed in the 5% and 10% $CO_2$ incubators. For cells with prior $CO_2$ treatment, the assay media was added just prior to transfection before being placed in the 5% and 10% $CO_2$ incubators for 20 hours. The TNF-$\alpha$ treatment was then given for 18 hours after this. Cells were lysed and the fluorescence measured.

### 2.6.6 Cell death

Cell death was estimated from samples transfected with the pRK5 vector or pRK5 vector containing K48R mutant ubiquitin. The cells were transfected for 18 and 36 hours. Media was aspirated from the wells and cells were resuspended with 100 $\mu$l of 1x PBS. The cells were mixed with 100 $\mu$l of 0.4% (w/v) Trypan Blue. Under a light microscope alive cells appeared white while dead cell membranes were stained blue after treatment with Trypan Blue. 5 $\mu$l of sample was pipetted onto a haemocytometer and the number of alive and dead cells were counted. The percentage of dead cells was then calculated from this.

# 3 - Results

The aim of this project was to test the hypothesis that mammalian cells exposed to elevated $CO_2$ levels downregulate the NF-κB pathway via reduced K48 polyubiquitination of IκBα. This was investigated using the NF-κB/293/GFP-Luc$^{TM}$ cell line which is derived from HEK 293 cells. These cells contain both a luciferase and GFP reporter driven by a minimal cytomegalovirus (mCMV) promoter. These reporters are downstream of four copies of the NF-κB consensus transcriptional response elements and upon activation of the NF-κB pathway there is transcriptional activation of the reporters. This leads to a Luc and fluorescence signal which can be easily detected and quantitatively measured as indicators of NF-κB activity (System Biosciences, 2018, https://www.systembio.com/wp-content/uploads/TR860_Web_Manual.pdf).

## 3.1 Preliminary results

To test if elevations in $CO_2$ downregulates NF-κB activation within the reporter cell line NF-κB/293/GFP-Luc$^{TM}$, a dose response to the inflammatory cytokine TNF-α was carried out at normocapnic (37 °C, 5% $CO_2$, 21% $O_2$) and hypercapnic conditions (37 °C, 10% $CO_2$, 21% $O_2$). TNF-α was used as this binds to the TNFR1 and activates the canonical NF-κB pathway (Figure 1.2).

After 18-hours of TNF-α and elevated $CO_2$ treatment there was a significant increase in NF-κB activation, measured by the Luc signal (Figure 3.1 C). The individual data points measured for the Luc signal varied quite widely (data not shown), and so once the luciferase substrate was mixed with the lysate sample, the signal was measured every 5 seconds for 30 seconds. An average signal was calculated across these 7 measurements.

The normality tests Anderson-Darling, Shapiro-Wilk and Kolmogorov-Smirnov all indicated the 10% $CO_2$ data was not normally distributed in Figure 3.1 C, and so the 95% confidence interval for the top values for each curve was compared. This

indicated these two data sets were significantly different (data not shown), and the Akaike Information Criterion (AIC) indicated that a different curve for each dataset was the best fit model. Discovering that elevated $CO_2$ caused a significant increase and not a decrease in NF-κB activity after an inflammatory stimulus was unexpected and contradicted many previous studies (Takeshita *et al.*, 2003; Cummins *et al.*, 2010; Wang *et al.*, 2010; Oliver *et al.*, 2012; Horie *et al.*, 2016). The transcription rate in mice skeletal muscle was reduced under hypercapnic conditions, with a significant reduction in protein synthesis (Caso *et al.*, 2005). Although this is *in vivo* in rat skeletal muscle, there may also be a reduction in transcription within the NF-κB/293/GFP/Luc at elevated $CO_2$ conditions. The protein content was used to normalise data and if the hypercapnic samples showed significantly reduced protein synthesis it could be enough to skew the data.

Previous studies incubated cells between 0.5-8 hours after LPS or TNF-α treatment (Takeshita *et al.*, 2003; Cummins *et al.*, 2010; Wang *et al.*, 2010; Oliver *et al.*, 2012; Masterson *et al.*, 2016), and so it was postulated that elevated $CO_2$ may delay the TNF-α-induced increase in NF-κB activation. Therefore, by 18 hours it is possible the 5% $CO_2$ but not the 10% $CO_2$ treated cells had successfully activated the negative feedback loop which prevents constitutive NF-κB activation (Wertz and Dixit, 2010). This may explain why at 18 hours the 10% $CO_2$ treated cells had elevated activity compared to the normocapnia treated cells. The same experiment was then carried out at 2 and 6 hours (Figure 3.1 A and B respectively). Despite a two-way ANOVA test indicating at 2 hours there was a significant reduction in activity at 10% $CO_2$ compared to normocapnia, the AIC analysis highlighted the best fit model for both datasets was one curve. Not only this, but the Luc signal was also 100 times lower compared to the 6- and 18-hour experiments; and so this result needs to be considered with caution. Especially as the same pattern was demonstrated in these two latter assays, and only a 2- and 5-fold increase for the 5% and 10% $CO_2$ conditions respectively between the 6-hour and 18-hour results at the highest dose. Whereas the comparison between the conditions at the highest dose for the 2-hour and 18-hour assay involved a 57- and 675-fold increase in activity for the 5% and 10% $CO_2$

47

respectively. This seems like too much of a dramatic increase in activity, and is probably due to a lack of a proper response by the cells at 2 hours.

As would be expected at a shorter time point, the Luc signal was lower at 6 than 18 hours but a clear signal was still produced. The Anderson-Darling, D'Agostino & Pearson, Shapiro-Wilk and Kolmogorov-Smirnov normality tests all indicated the 6-hour data was normally distributed; and the two-way ANOVA test showed a significant elevation in the Luc signal at 10% $CO_2$. The elevation and not reduction in NF-$\kappa$B signal at 10% $CO_2$ seen at 6 hours, indicated that the elevation seen here and reduction seen elsewhere (Cummins *et al.*, 2010; Oliver *et al.*, 2012; Masterson *et al.*, 2016) was not caused by measuring the NF-$\kappa$B activity at different timepoints. Therefore the methodology was further investigated.
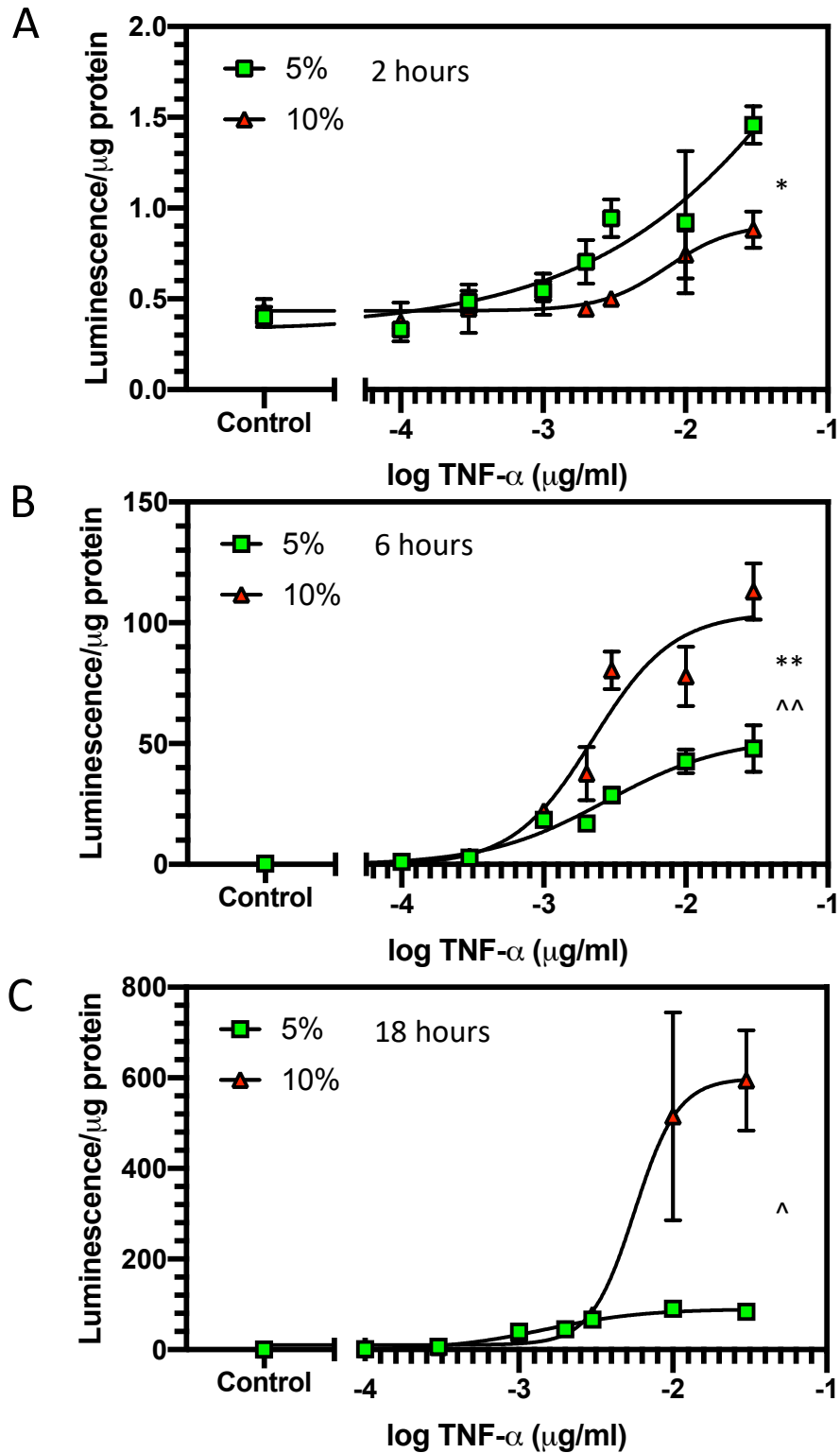
**Figure 3.1**

Elevated $CO_2$ increased NF-κB activation after TNF-α treatment on cells. A) Luc signal at 5% and 10% $CO_2$ after 2 hours of TNF-α treatment. B) Luc signal at 5% ad 10% $CO_2$ after 6 hours of TNF-α treatment. C) Luc signal at 5% and 10% $CO_2$ after 18 hours of TNF-α treatment (0.1-30 ng/ml). Control data points were cells treated with PBS and incubated for the same period as the TNF-α. 'Original Media' from Table 2.1. The Luc signal was normalised to μg of protein. Error bars show standard deviation. N=3. Two-way ANOVA * $p < 0.01$, ** $p < 0.0001$. AIC analysis ^ $p < 0.01$, ^^ $p < 0.0001$.

## 3.2 Method development

The unexpected finding that elevated $CO_2$ caused an increase and not a reduction in NF-κB activation, led to a series of experiments to test if the signal measurement, media pH or the specific cell line used were impacting on the NF-κB activity output.

The individual Luc signal measurements varied widely both between biological replicates and within the same sample across the 30 seconds of signal measurement. Due to the nature of the Luc signal, to prevent variation in the delay between the addition of the substrate to the sample and then subsequent luminometry reading, all samples were measured individually rather than adding substrate to several samples and then measuring them all. It was then hypothesised that due to the large variation within the data the true NF-κB output was not being accurately represented. To determine the signal profile the Luc signal was measured every 2 seconds for 30 minutes (Figure 3.2). Over this period the signal gradually decayed and there was large variation in the Luc signal across the whole 30 minutes. Although the signal was quite noisy it remained fairly stable for the first 5 minutes (marked on the graph) before slowly decaying. Indeed this evidence would indicate the Luc signal could have been 'masking' the true NF-κB output. To prevent this factor from impacting overall trends, in further assays the Luc signal was then measured every 16 seconds for 5 minutes and an average signal was calculated.
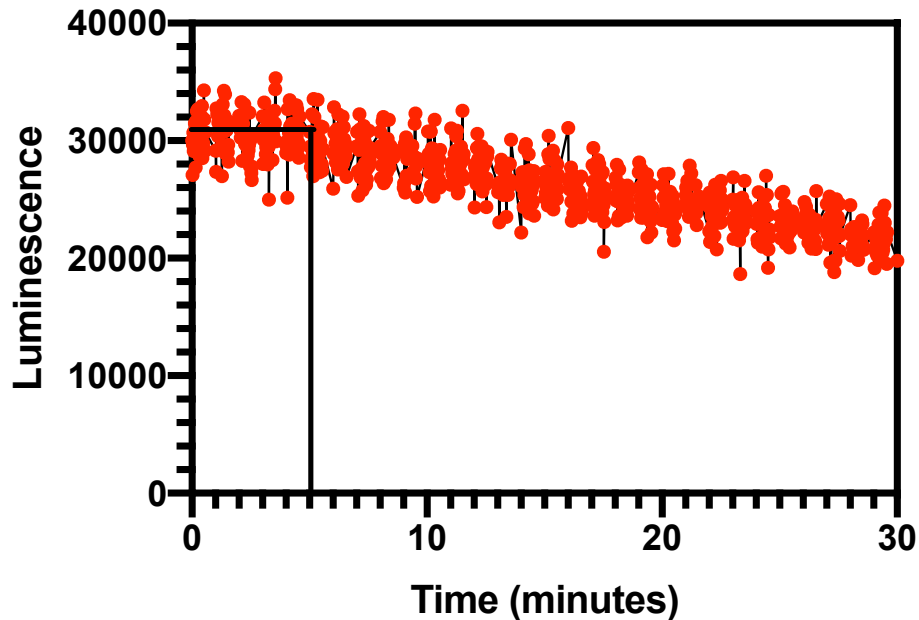
**Figure 3.2**
The Luc signal decayed over 30 minutes. The Luc signal was measured every 2 seconds for 30 minutes after the luciferase substrate was mixed with sample lysate from cells treated with 30 ng/ml of TNF-$\alpha$ for 18 hours. The signal remained stable for the first 5 minutes, marked on the graph, before there was a gradual decay in the signal. Raw Luc signal.

Using this potentially more accurate method for measuring the Luc signal, the 6-hour assay was repeated (Figure 3.3 A). However, this resulted in a loss in the difference seen between the $CO_2$ treatments. As the normality tests Anderson-Darling, D'Agostino & Pearson, Shapiro-Wilk and Kolmogorov-Smirnov all highlighted the data was normally distributed a two-way ANOVA test was used. This showed there was no significant difference between the $CO_2$ groups, and similarly the AIC analysis highlighted the best fit model was one curve for both datasets. The assay was the repeated but at 18 hours (Figure 3.3 B). The Anderson-Darling, D'Agostino & Pearson, Shapiro-Wilk and Kolmogorov-Smirnov normality tests all indicated the 18-hour data was normally distributed; and both the two-way ANOVA and AIC analysis indicated the two data sets were significantly different. When an average Luc signal over 5 minutes was measured there was no change to the overall trend, and increasing the $CO_2$ to 10% still caused a significant increased to the TNF-$\alpha$-induced activation of the

NF-κB pathway. Therefore, calculating an average signal over 5 minutes does not appear to explain this trend.
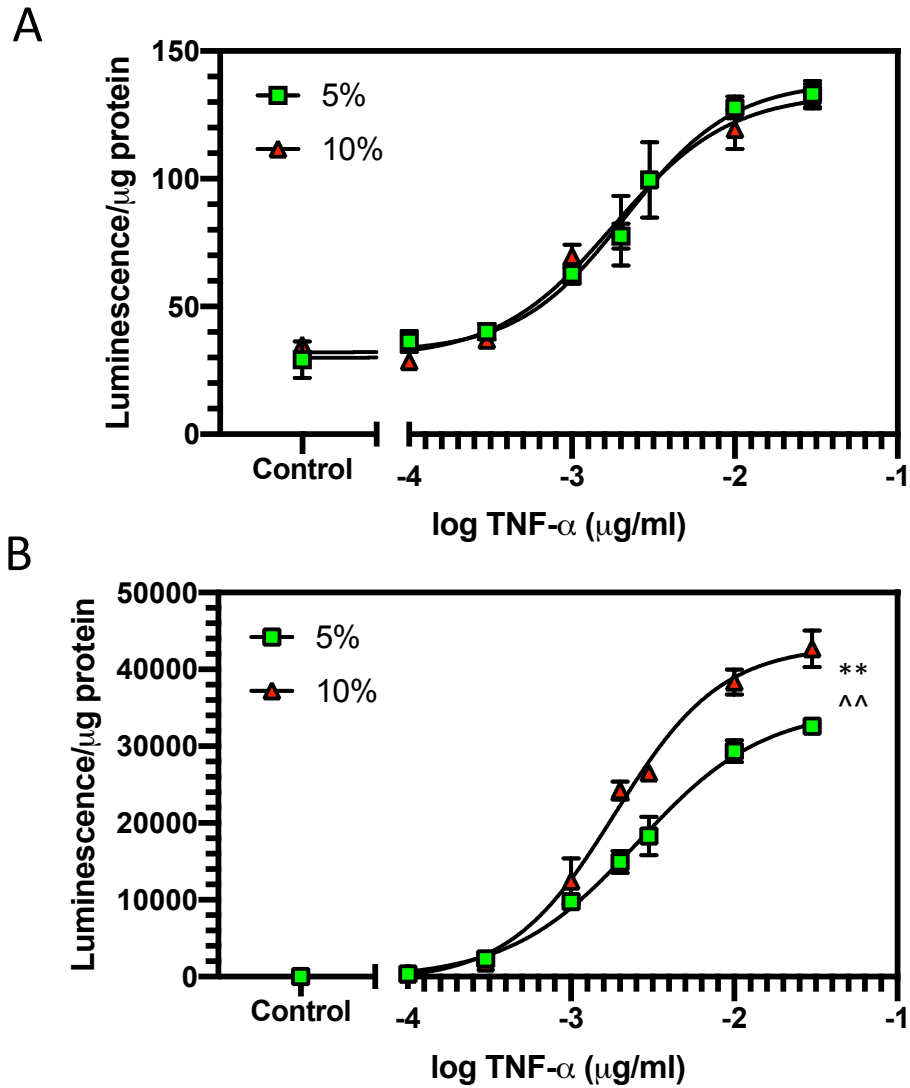
**Figure 3.3**

Measuring and averaging the Luc signal over 5 minutes reduced data variability. However it did not change the significant increase in Luc signal at 10% $CO_2$ after TNF-$\alpha$ treatment (0.1-30 ng/ml). A) Luc signal at 5% and 10% $CO_2$ after 6 hours of TNF-$\alpha$ treatment. B) Luc signal at 5% and 10% $CO_2$ after 18 hours of TNF-$\alpha$ treatment. The control were PBS treated cells for the same period at TNF-$\alpha$ treatment. 'Original Media' from Table 2.1. The Luc signal was normalised to $\mu$g of protein. Error bars show standard deviation. N=3. Two-way ANOVA ** $p < 0.0001$. AIC analysis ^^ $p < 0.0001$.

### 3.2.1 pH experiments

Reductions in pH have been shown to either influence or even be the primary cause for cytokine-induced alterations in NF-κB activation after elevations in $CO_2$ levels (Takeshita *et al.*, 2003; O'Toole *et al.*, 2005; Horie *et al.*, 2016). If the effects of elevated $CO_2$ were mediated by the secondary pH reductions and there were differences in the media pH across the hypercapnia and normocapnia groups, then the media pH could be influencing the overall NF-κB activity.

To see if there were differences in media pH across treatment groups, media was incubated overnight at ambient, 5% and 10% $CO_2$ before placement on cells at these conditions. The pH was measured before and after 8 hours on cells (Figure 3.4). At all three conditions there was a significant increase in pH after the media had been placed on the cells. This result was unexpected as placement onto cells should normally cause a reduction in pH due to the excretion of acidic metabolites by the cells. Media samples were extracted, placed into falcon tubes and then sealed before the pH was measured, this delay may have impacted on the pH readings and caused these unusual results. To counteract the usual acidification of media caused by cellular acidic metabolites the alkaline sodium bicarbonate is added to media. With increasing $CO_2$ there is also an expected acidification of media due to the increased production of $H^+$, and therefore the media levels of sodium bicarbonate were stepwise increased for the ambient to 10% $CO_2$ media, based on previous work (Oliver *et al.*, 2012) (See Table 2.1 'Original media'). The level of buffering capacity of the sodium bicarbonate added to the different conditions would appear far greater than what was needed to level the media pH across conditions, and would likely explain why there was a stepwise increase in pH despite the increase in $CO_2$ concentrations.

The pH was not measured for the assays in Figures 3.1 and 3.3, and so the pH for the 5% condition could have been lower compared to the 10% as seen in Figure 3.4. If the reduction in NF-κB activity caused by elevations in $CO_2$ are due to the secondary effects of reduced pH under the experimental conditions used, this may explain why

the 10% assays appeared to show elevated activity. Therefore, an assay was carried out comparing the effect of reducing the pH after TNF-$\alpha$ treatment for 18 hours. There was a significant reduction in TNF-$\alpha$-induced NF-$\kappa$B activation at both 5% and 10% $CO_2$ when media pH was reduced (Figure 3.5). The decrease in pH was achieved by reducing the sodium bicarbonate levels within the media. Therefore, under these experimental conditions lowering the media pH by adding less sodium bicarbonate caused a reduction in NF-$\kappa$B activity in NF-$\kappa$B/293/GFP-Luc$^{TM}$, and so pH may have been the cause for the increase in activity at 10% $CO_2$ relative to the normocapnic conditions.

Interestingly, there was still a significant increase in activity at 10% $CO_2$ compared to 5% $CO_2$ after TNF-$\alpha$ treatment, when the media pH was at a more physiological level (pH 7.52 for the 5% $CO_2$ and pH 7.42 for the 10% $CO_2$) (Figure 3.5). The reduction in pH in the conditions which showed a significant reduction in NF-$\kappa$B activity was far greater than the differences in pH seen between the 5% and 10% $CO_2$ conditions (Figure 3.4). As seen in previous studies reductions in pH at normocapnia can reduce NF-$\kappa$B activity, but the level at which the pH was dropped was much larger than that seen by hypercapnia acidosis (Wang *et al.*, 2010). Therefore, to test if there was still a reduction in NF-$\kappa$B activity at smaller pH reductions, media pH was reduced from 7.44 to 7.08 at both 5% and 10% $CO_2$ by altering the sodium bicarbonate levels (Figure 3.6). A one-way ANOVA indicated there was no significant difference across this pH range, which was also found in the human THP-1 and monocyte derived macrophage cell lines when the media pH was only reduced to pH 7 (Gerry and Leake, 2014). Although there was a trend for increased activity at the 10% $CO_2$ condition compared to 5% $CO_2$, there was not a significant increase in NF-$\kappa$B activity. This would indicate that pH and $CO_2$ are acting via difference mechanisms, as reductions in NF-$\kappa$B activity caused by pH are at a far lower pH than that seen by hypercapnia acidosis.

To ensure that pH was not a contributing factor to the differences in NF-$\kappa$B activity seen between 5% and 10% $CO_2$ treated cells, subsequent assays had the media pH

measured and controlled. Different amounts of sodium bicarbonate were added to the 5% and 10% $CO_2$ media to achieve the same pH by the end of the assay (see Table 2.1 'Assay Media' for specific sodium bicarbonate levels).

If it is only the larger reductions in pH which influences NF-$\kappa$B activity, then controlling for the small differences in pH across the 5% and 10% $CO_2$ media would not change the trend seen previously, that elevated $CO_2$ increases activity. A dose response was then carried out which controlled the pH at both $CO_2$ conditions (Figure 3.7). When the pH was controlled, 10% $CO_2$ still caused a significant elevation in NF-$\kappa$B activation after TNF-$\alpha$ stimulation. As the data was normally distributed according to the Anderson-Darling, D'Agostino & Pearson, Shapiro-Wilk and Kolmogorov-Smirnov tests, a two-way ANOVA was carried out. This indicated there was a small but significant increase at 10% $CO_2$ compared to normocapnia ($p < 0.05$). Similarly, an AIC analysis indicated the best fit model was two separate curves for the 5% and 10% $CO_2$ data. This finding would indicate that elevated $CO_2$ causes an increase in NF-$\kappa$B activity, and that the small differences in pH between 5% and 10% $CO_2$ were not the cause for the differences seen in NF-$\kappa$B activity. However, controlling the pH appeared to reduce the clear cut differences in activity seen across the conditions as seen previously (Figures 3.3 B). There was large variation within the dataset which is clearly shown by the wide and overlapping error bars (Figure 3.7). Little previous evidence indicates that elevating $CO_2$ causes an increase in cytokine-induced stimulation of the NF-$\kappa$B pathway. Therefore, another reporter cell line was used to investigate if this finding was due to experimental design or potentially a unique response discovered in this specific cell line.
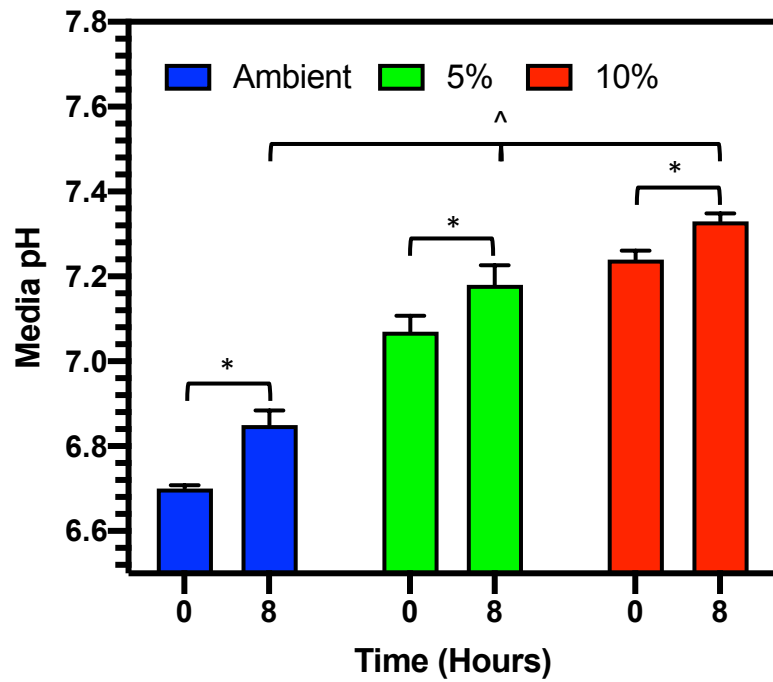
**Figure 3.4**

Media pH was significantly altered after 8 hours on cells at both ambient and 10% $CO_2$. 'Original Media' from table 2.1. Error bars show standard deviation. N=3. T Test 0 vs 8 hours for that $CO_2$ condition * $p < 0.05$. T Test compared to 8 hour pH at 5% $CO_2$ ^ $p < 0.01$
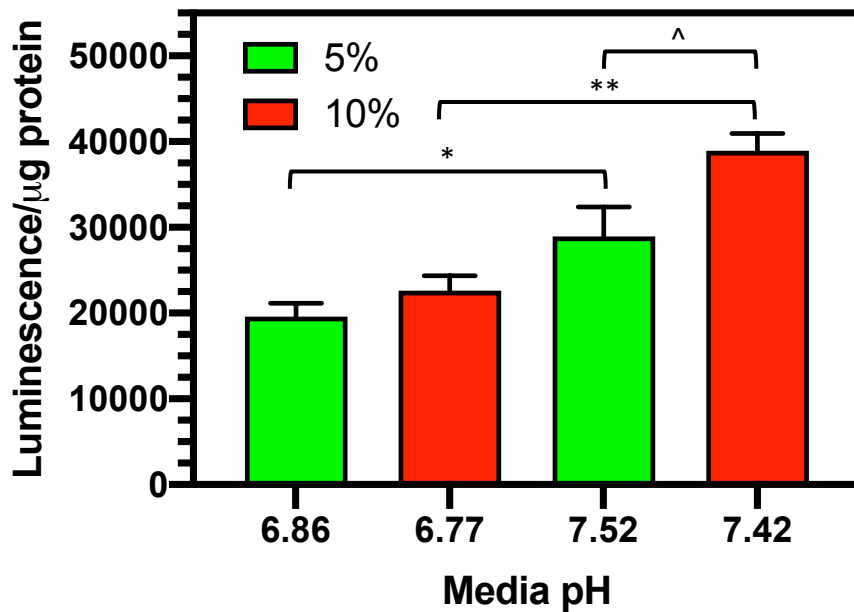


**Figure 3.5**

Dropping the media pH at both 5% and 10% $CO_2$ significantly reduced the TNF-$\alpha$-induced NF-$\kappa$B activation. The cells were stimulated with 30 ng/ml TNF-$\alpha$ for 18 hours. Media pH reduced by reducing sodium bicarbonate levels. Error bars show standard deviation. N=3. T Test compared condition to lower pH * $p < 0.05$ ** $p < 0.001$. T Test compared 5% and 10% at the higher pH ^ $p < 0.05$.
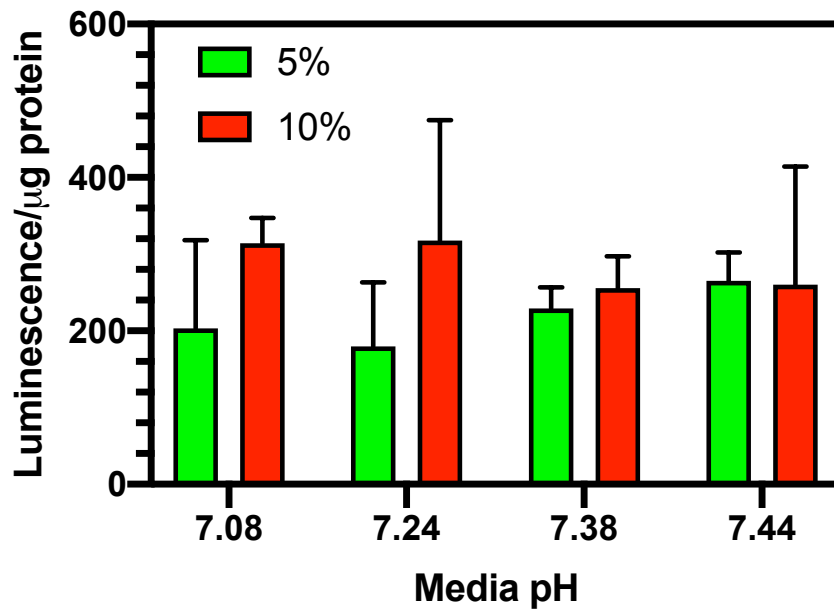
**Figure 3.6**
Reducing the media pH from 7.44 to 7.08 did not cause a significant alteration to NF-κB activity. Stimulated with 30 ng/ml TNF-α for 18 hours. Luc signal was normalised to μg of protein. pH altered through altering sodium bicarbonate levels. Error bars show standard deviation. N=3.
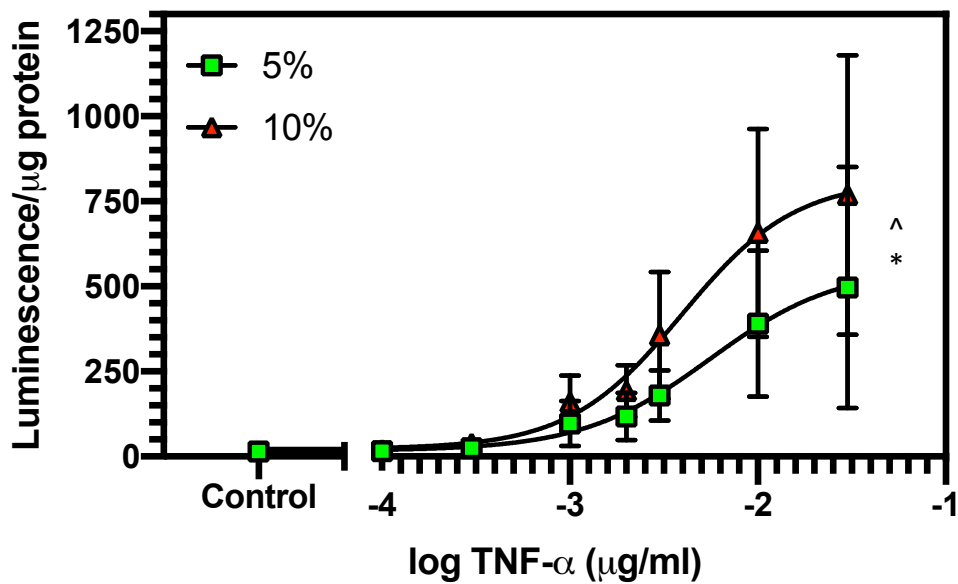


**Figure 3.7**
Elevating $CO_2$ levels to 10% significantly increased the TNF-α-induced activation of the NF-κB pathway. Luc signal after 18 hours of TNF-α (0.1-30 ng/ml). The control data points were PBS treatment for 18 hours. 'Assay Media' from Table 2.1. Error bars show standard deviation. N=12. Two-way ANOVA * $p < 0.05$. AIC ^ $p < 0.01$.

### 3.2.2 U251-NF-κB-GFP-Luc cell line

To test the experimental design of the assay the human U251-NF-κB-GFP-Luc cell line was also tested. This cell line was derived from brain tissue of a grade III-IV malignant astrocytoma tumour, and is an ideal cell line for investigating inflammatory responses (Zeuner *et al.*, 2017). This cell line has been stably transduced with the lentiviral NF-κB-driven tandem reporter, which like the NF-κB/293/GFP-Luc$^{TM}$ cell line, contains both a Luciferase and GFP reporter. Therefore, upon stimulation with TNF-α there would be both an increase in NF-κB activation and Luc and fluorescence signal, allowing for the easy detection of NF-κB activation.

An initial TNF-α dose response was carried out on the U251-NF-κB-GFP-Luc cell line for 6 hours (Figure 3.8 A). As seen with the NF-κB/293/GFP-Luc$^{TM}$ at 6 hours (Figure 3.3 A), there was not a significant difference between the 5% and 10% $CO_2$ conditions. The normality tests Anderson-Darling, D'Agostino & Pearson, Shapiro-Wilk and Kolmogorov-Smirnov indicated both data sets were normally distributed. The two-way ANOVA analysis indicated the 5% and 10% $CO_2$ conditions were not significantly different. However, an AIC analysis indicated the best fit model for the two data sets are two curves; and T Tests comparing the control values (0 ng/ml) with the TNF-α doses at 30, 10, 2 and 0.3 ng/ml indicated there was a small but significant NF-κB response to the cytokine.

As there was not a clear response to the TNF-α treatment, a dose response was then carried out for a longer time point and using higher TNF-α doses (Figure 3.8 B). There was still no response to the cytokine even at a dosage 10 times above that used to select the cell line (Zeuner *et al.*, 2017). This apparent lack of any response to the cytokine at 18 hours would indicate that at this stage the cells had mutated so the reporters no longer responded to changes to the NF-κB pathway activation. Although the passage number was not especially high (less than 10), it is possible that the freezing and thawing process damaged the cells, or even that the cell line had mutated prior to the freezing process. Not only this, but genotypic changes were seen even at fairly low passages (up to 10) and in the presence of the selection

59

antibiotic puromycin (which was not used within this study) by the group which developed the cell line (Zeuner *et al.*, 2017). Unfortunately, due to the restraints of this project there was not enough time to investigate this further, but a mutation in the cell line would seem the most likely reason for the lack of response to cytokine stimulation. If the projected had allowed then an enzyme-linked immunosorbent assay (ELISA) could be carried out to determine the presence of the reporter.
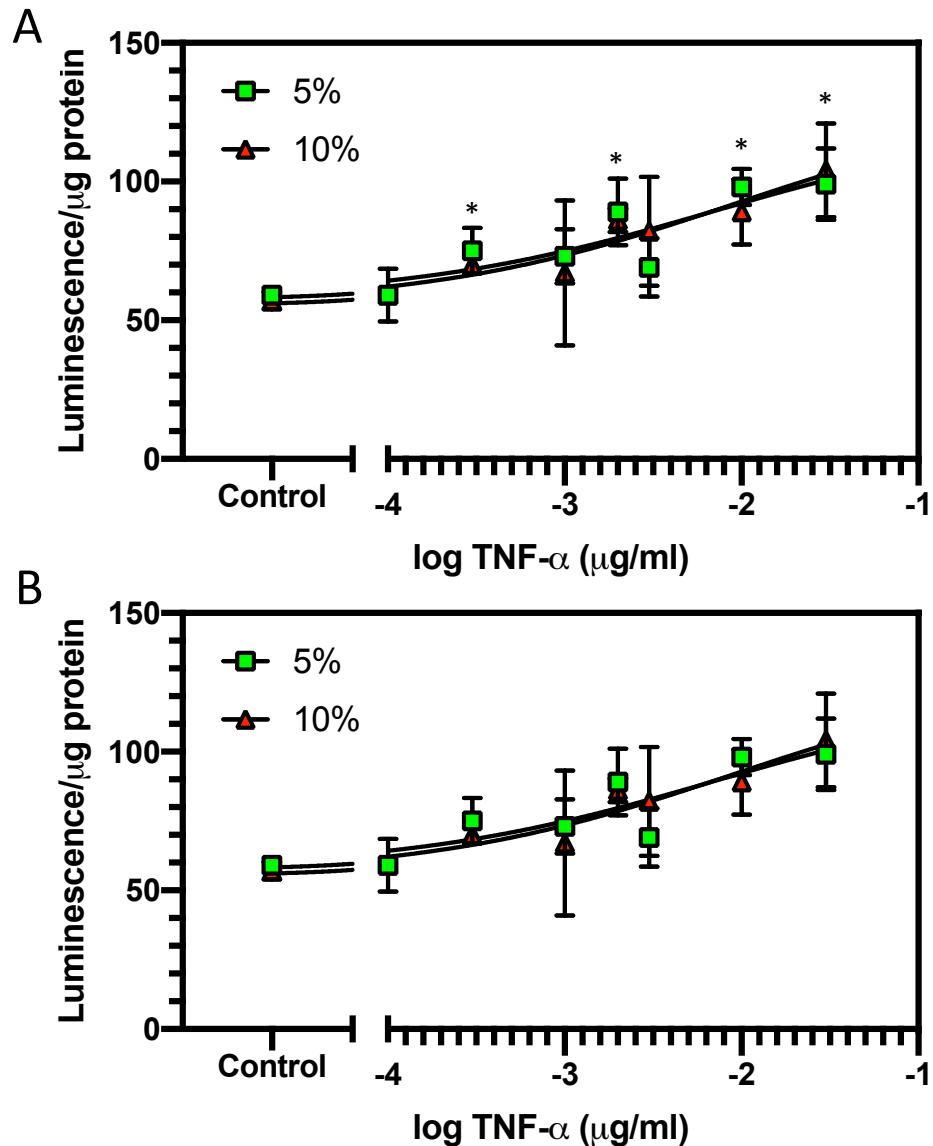


**Figure 3.8**
The U251-NF-$\kappa$B-GFP-Luc cell line did not response to TNF-$\alpha$ treatment. A) 6 hours of TNF-$\alpha$ treatment (0.1-30 ng/ml) at 5% and 10% $CO_2$. B) 18 hours of TNF-$\alpha$ treatment (1-100 ng/ml) at 5% and 10% $CO_2$. Control was PBS treatment for the same time as TNF-$\alpha$ treatment. 'Assay Media' from Table 2.1. Error bars represent standard deviation. N=3. T Test significantly different from the control * $p < 0.05$.

### 3.2.3 LPS

Many studies investigating the effect of hypercapnia on the NF-κB pathway stimulate cells with LPS. Although both LPS and TNF-α stimulate the canonical pathway they activate the IKK complex via a different receptor and signalling molecules (see Figure 1.4). Therefore, the effect of $CO_2$ may be affecting one of the molecules along the LPS and not the TNF-α pathway and may explain the unexpected results seen in this study. However, LPS binds to TLR4, and as HEK 293 cell line does not possess TLRs (Zeuner *et al.*, 2017) this could not be tested in the NF-κB/293/GFP-Luc$^{TM}$ cell line as a reason for seeing an elevation and not a decrease in NF-κB activity. Although other factors like IL-1 would have been a good alternative activator of the canonical pathway, LPS is much cheaper and more widely tested in the context of hypercapnia.

### 3.2.4 Luciferase vs GFP

As pH, cell line and stimulus for the pathway do not help to explain the unexpected findings of hypercapnia increasing NF-κB activity, the method for detecting NF-κB activation was investigated. Due to the unstable nature of the Luc signal after mixing the cell lysate with the luciferase substrate, the fluorescence signal was tested. As with the Luc signal (Figure 3.2), the fluorescence was measured every 2 seconds for 30 minutes (Figure 3.9). The fluorescent signal showed a much slower decay and much more stable signal in comparison. This is similar to previous findings, which have shown that although luciferase is much more sensitive than GFP the error rates are significantly larger (Close *et al.*, 2011). Over the first 5 minutes the range for the Luc signal was 34% of the average signal, whereas the range for the fluorescent signal was only 5% of the average. Similarly, the final 5-minute average had only decayed by 15% for the fluorescence compared to 27% for the Luc signal. Figure 3.10 helps to visualise the unstable nature of the Luc signal in comparison to the fluorescence signal. It shows the ratio of the maximal signal detected within the first 5 minutes of both the Luc and fluorescence signal from samples stimulated with 30 ng/ml of TNF-α.
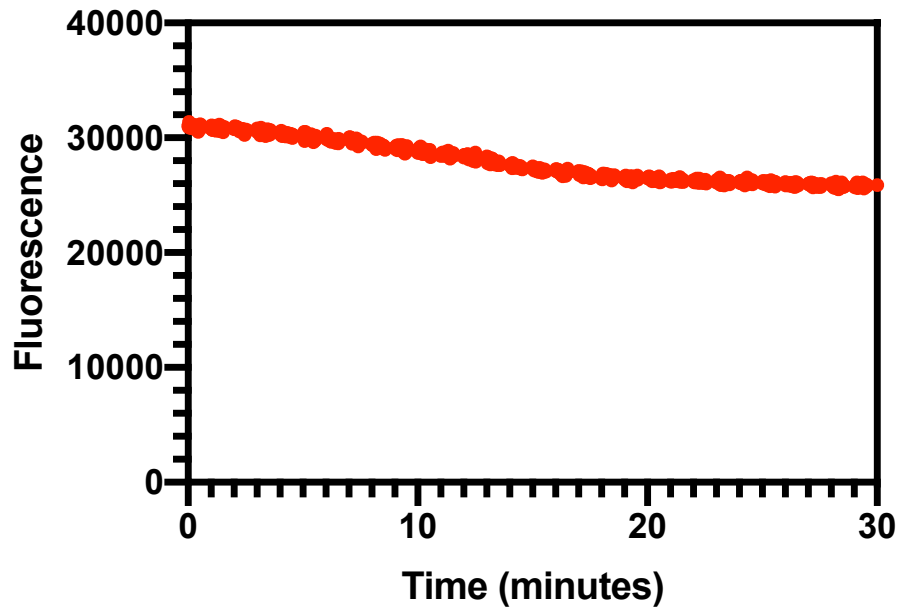
**Figure 3.9**
The fluorescent signal remained stable and showed little photobleaching over the 30 minute period. The fluorescence was measured every 2 seconds for 30 minutes from cellular lysate treated with 30 ng/ml of TNF-$\alpha$ for 18 hours.
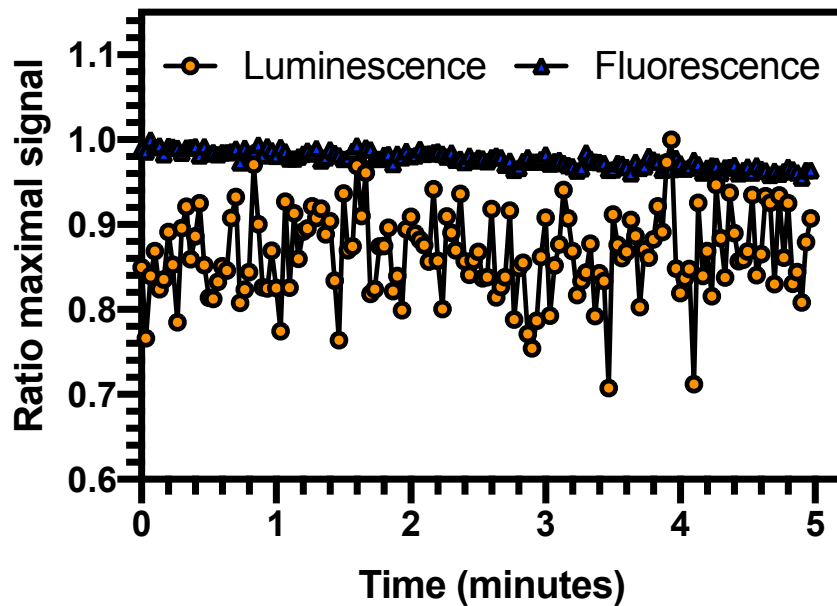


**Figure 3.10**
The fluorescence signal was much more stable than the Luc signal over the first 5 minutes. Tracks the ratio of the raw maximal signal detected over the first 5 minutes for both the Luc and fluorescence signals.

The half-life of GFP and luciferase are similar, at 2 and 3 hours respectively; and have similar sensitivities as reporters (Ducrest, 2002). However, to obtain a Luc signal from the luciferase enzyme the addition of ATP, $Mg^{2+}$, $O_2$ and luciferin are required (Thompson, Hayes and Lloyd, 1991). This meant that cellular lysate samples had to be mixed with these to obtain a signal, adding an additional step to the protocol. On the other hand, the GFP fluorophore forms spontaneously intracellularly without the need for the addition of a cofactor (Ducrest, 2002). Due to the high number of samples in the dose response assays the addition of the substrate for the Luc signal had to be staggered, delaying the signal detection for certain samples. This may have led to the degradation of some of the luciferase enzyme, affecting the overall Luc signal; whereas all the samples could be measured at one time when measuring the GFP signal. So, although the previous results indicated that elevating $CO_2$ caused an increase in NF-κB activation, findings based on the Luc signal alone should be considered with caution.

The noisy nature of the Luc signal could therefore be affecting the accuracy of the data collected previously (as can be clearly seen in Figure 3.10). Therefore, to test if the Luc signal was affecting the overall outcome for detecting differences between 5% and 10% $CO_2$, a comparison was made between the two signals based from the same lysate sample treated with 1x PBS or 30 ng/ml of TNF-α (Figure 3.11). Indeed no significant difference was seen between the 5% and 10% at 30 ng/ml for the Luc signal (Figure 3.11 A), but the 10% signal was significantly lower than the 5% for the fluorescent signal (Figure 3.11 B). Therefore, the Luc signal appeared to be a likely cause for the 10% $CO_2$ data appearing to show an elevation in NF-κB activity compared to normocapnia conditions.
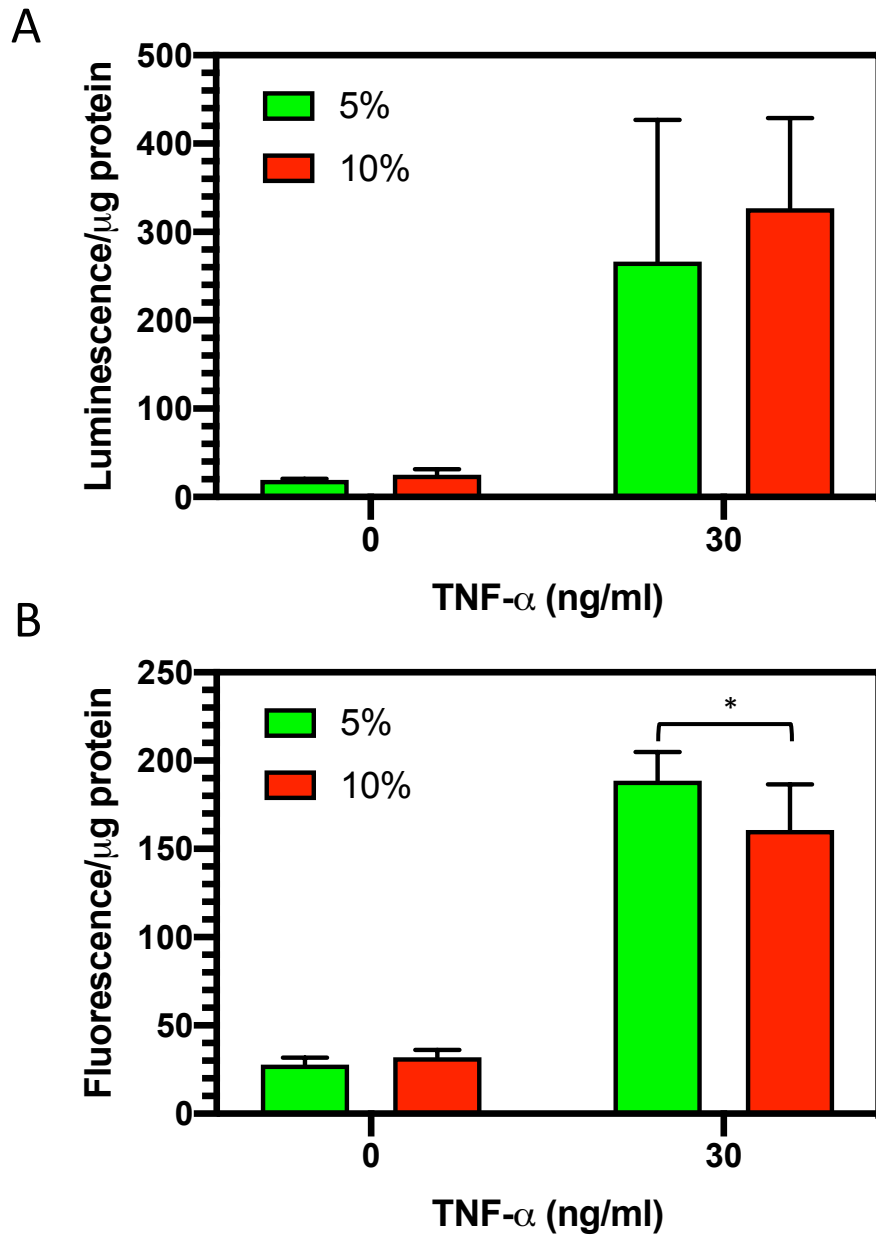
**Figure 3.11**
The Luc signal was too unstable to get reliable results compared to the fluorescence. A) Luc signal after cells had been treated with PBS or 30 ng/ml of TNF-α for 18 hours. B) Fluorescent signal measured from the same sample as seen in (A). 'Assay Media' from Table 2.1. Error bars represent standard deviation. N=18 for 30 ng/ml dose and N=6 for 0 ng/ml TNF-α. T Test * *p* < 0.001.

In summary, due to these findings sodium bicarbonate was used to control pH levels of the media at both 5% and 10% $CO_2$ (see Table 2.1 'Assay Media'). For subsequent assays the fluorescence signal was measured instead of the Luc signal. Although calculating an average signal from the first 5 minutes of the Luc signal produced better results, it would appear the noisy nature of the signal meant the results were still unreliable.

## 3.3 Testing the hypothesis

The main objective of this project was to test the hypothesis that elevated $CO_2$ causes carbamylation at lysine residue 48 of ubiquitin, preventing K48 polyubiquitin chain formation. This would then prevent the breakdown of the canonical pathway inhibitor I$\kappa$B$\alpha$, so the NF-$\kappa$B subunits are held within the cytoplasm and do not activate transcription. Therefore, carbamylation is more likely at elevated $CO_2$ levels and cause the shutdown of the pathway.

To begin to test this hypothesis, cells were transfected with ubiquitin DNA which had individual lysine residues mutated to an arginine. Lysine and arginine have similar structural and chemical properties, and are both positively charged polar amino acids, but the mutation to an arginine prevents the formation of polyubiquitin chains (Finley *et al.*, 1994). This method would not only block I$\kappa$B$\alpha$ degradation, but the many other pathways regulated by the addition of the different lysine linked polyubiquitin chains. However, this method was a good place to start testing the hypothesis due to the fairly straight forward methodology. The DNA was packaged within a pRK5 vector which contained a CMV promoter, allowing the stable and constitutive expression of the mutant ubiquitin (Foecking and Hofstetter, 1986; Lim *et al.*, 2005). Cells transfected with these vectors would be flooded with the mutant ubiquitin. This meant the mutant would outcompete the endogenous ubiquitin, and so the transfected cells effectively acted as a mutant ubiquitin cell line. There is the possibility the activity of the CMV promoter could be altered by transcription factors within the cell, for instance p53 and MAP/ERK kinase kinase 1 are known down- and

up-regulators respectively of the CMV promoter (Rodova *et al.*, 2013). It was assumed these would not impact on the results in the subsequent assays.

Cells were transfected with ubiquitin mutants and then treated with TNF-$\alpha$ at both normocapnic and hypercapnic conditions. However, preliminary findings indicated the transfection process was affecting cellular growth and survival. It was then determined to find time points that allowed successful DNA transfection when cells began the TNF-$\alpha$ treatment, but did not result in excessive cell death by the end of the assay. To test the transfection efficiency cells were transfected with GFP. This allowed the easy detection of protein production via the fluorescent signal whilst also giving an indication of the timescale for successful transfection. Fluorescence was observed after 18 and 36 hours, but the signal was significantly lower at 18 hours (Figure 3.12 A). The effect on cell growth/death of the transfection reagents alone was not tested.

The cell injury and therefore a marker for cell death was also determined by treating samples with trypan blue. This dye does not colour cells that are alive and healthy but colours dead or damaged cell membranes blue. Using this method cell viability was estimated at both 18 and 36 hours for cells transfected with the pRK5 vector alone or containing the K48R ubiquitin mutant (Figure 3.12 B). There was a significant reduction in cell viability between 18 and 36 hours for both the vector and K48R ubiquitin mutant. However, there was no significant difference found between the vector and K48R at both 18 and 36 hours. This meant that comparisons made between controls containing the vector and mutant ubiquitins could be made without the need to account for differences in the number of viable cells. The comparison was made with the vector alone and not with wild type ubiquitin, as this was not currently available within the lab at the time of the assays.

To ensure the transfected DNA was being expressed to sufficient levels, subsequent transfection assays involved transfection for 20 hours prior to TNF-$\alpha$ stimulation.
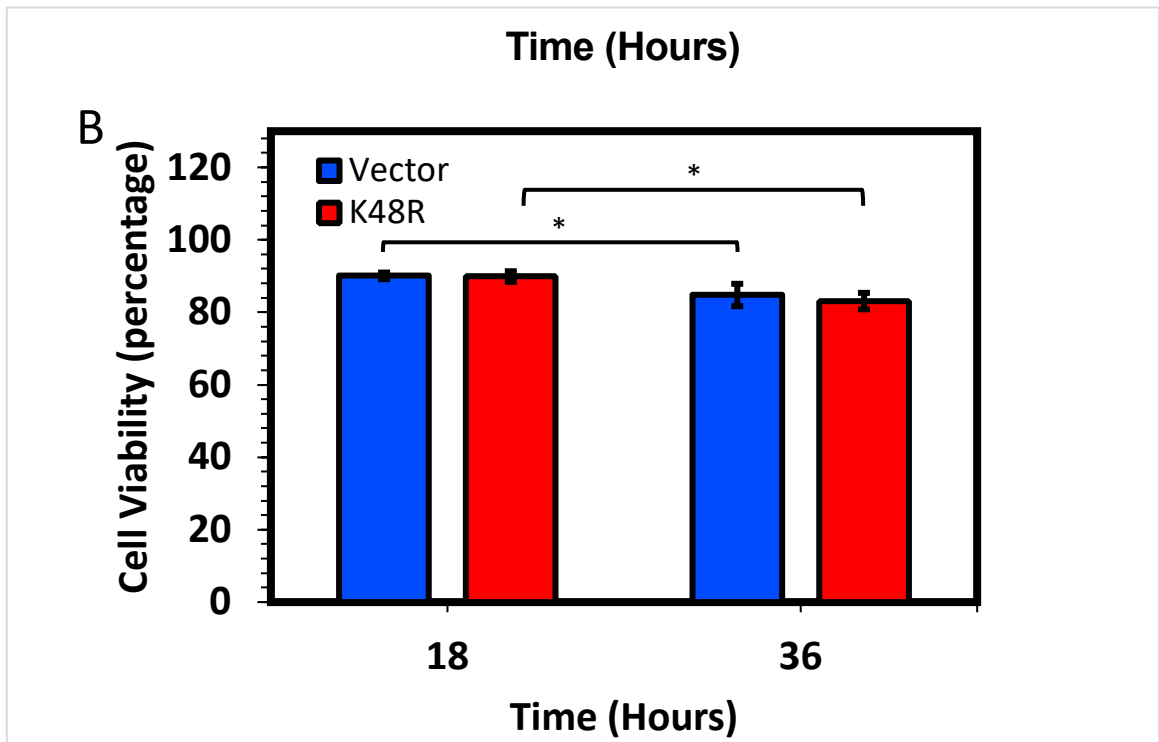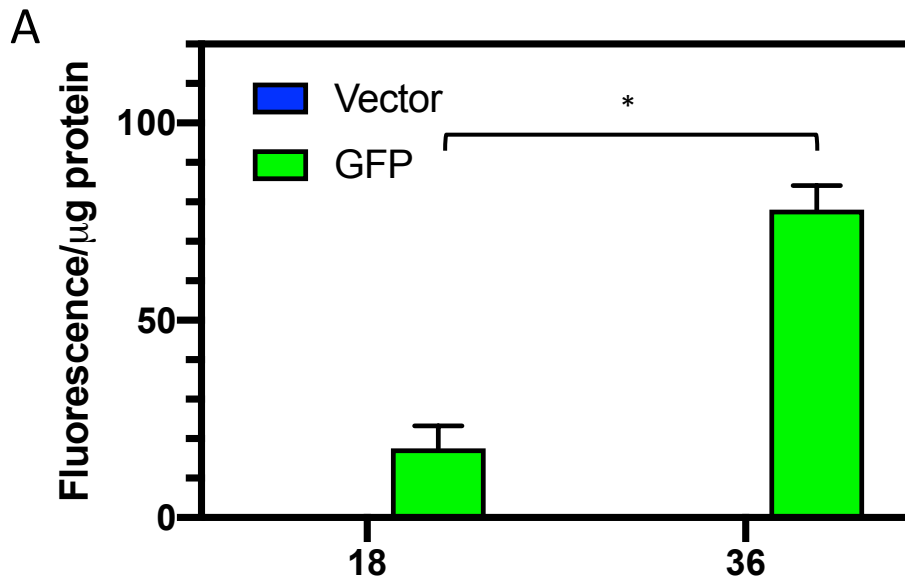
**Figure 3.12**
After 18 hours successful transfection of DNA had occurred and cell death increased over time after transfection with DNA. A) Cells were transfected with an empty pRK5 vector (vector) or vector containing GFP (GFP), and the fluorescence was measured after 18 and 36 hours. The fluorescence was normalised to μg of protein. B) Cell viability after transfection with the empty pRK5 vector or pRK5 vector containing the K48R ubiquitin mutant (K48R). 'Assay Media' from Table 2.1. Error bars represent standard deviation. N=3. T Test comparing 18 and 36 hour time point * $p < 0.05$

To test the main hypothesis that carbamylation occurs at K48R and prevents K48R polyubiquitination, cells were transfected with K48R and activated with TNF-$\alpha$ (Figure 3.13 A). A significant reduction in activity at 10% $CO_2$ compared to 5% $CO_2$ was seen, indicating that the vector itself did not interfere with the effect of elevated $CO_2$ on NF-$\kappa$B activity. Cells transfected with the mutant showed a significant reduction in activity compared to the vector when both were treated with 30 ng/ml of TNF-$\alpha$ for 18 hours. It is well known that K48 polyubiquitination is important for canonical NF-$\kappa$B activation (Wertz and Dixit, 2010), and reductions in activity seen with the mutant validates the transfection methodology. However, the most interesting finding from this assay, was there was no difference in the activity seen between the 5% and 10% $CO_2$ treatments for the K48R mutant when stimulated with TNF-$\alpha$. As the elevation in $CO_2$ does not cause any further reductions in activity, it would indicate that the mutant occluded the effects of elevated $CO_2$ on NF-$\kappa$B activation. Although this does not provide conclusive evidence that carbamylation is occurring at K48 and this is the reason for the NF-$\kappa$B pathway shutdown, it does not disprove the original hypothesis.

The K48R mutant did not cause a complete blockade of the NF-$\kappa$B pathway, and there was still a significant increase in activity at 30 ng/ml of TNF-$\alpha$ compared to the 0 ng/ml control at both 5% and 10% $CO_2$. This incomplete blockade of the pathway could be due to several reasons. Firstly, that the K48 polyubiquitin chains are not essential for the activation of the canonical pathway. Secondly, as the assay involved flooding the system with a mutant rather than knocking out the endogenous production of ubiquitin, the endogenous ubiquitin could have activated the pathway and caused some background activation. Thirdly, the transfection efficiency was not tested in each assay and as 100% transfection efficiency is unlikely, some cells may have produced a baseline activation of the pathway.

To test if overnight incubation of cells at the elevated $CO_2$ levels altered the responses, the cells were incubated at 5% or 10% $CO_2$ at the time of infection (Figure 3.13 B). The cells were placed at the elevated $CO_2$ at the time of transfection, this

reduced the time in which the cells were out of the 10% $CO_2$ incubator during the experiment, meaning the cells were exposed to 10% $CO_2$ for 20 hours prior to the addition of TNF-$\alpha$. The media pH was measured before addition onto cells, after 20 hours of incubation on cells and at the end of the assay, and at all time points the media pH was the same across the 5% and 10% $CO_2$ treatments. As seen without the pre-incubation of the cells, there was a significant reduction in NF-$\kappa$B activity at elevated $CO_2$ levels with cells transfected with the vector. However, there was only a significant reduction in activity at 30 ng/ml of TNF-$\alpha$ at 5% and not at 10% $CO_2$ for the K48R mutant compared to the K48R treated with 0 ng/ml of TNF-$\alpha$. This could indicate that the pre-incubation of cells had a more powerful effect at reducing the NF-$\kappa$B activity and blocked the effect of TNF-$\alpha$ more effectively when there was prior incubation at 10% $CO_2$. The mutant did not increase any reductions on top of hypercapnia, as seen in Figure 3.13 A. However, the lack of a significant increase in activity at 30 ng/ml of TNF-$\alpha$ with the K48R mutant could be an indication the TNF-$\alpha$ was not working properly. As the same TNF-$\alpha$ was used for the vector at 30 ng/ml this would seem an unlikely cause for the effects seen in Figure 3.13 B. The overall fluorescence signal to the TNF-$\alpha$ were lower than that seen in Figure 3.13 A, and could indicate the cells were not properly responding to the cytokine. It would appear that prior incubation of cells at elevated $CO_2$ has a more powerful effect at reducing cytokine-induced activation of NF-$\kappa$B, however this assay would need to be repeated to ensure these effects are not due to a mutation in the reporter cell line.

K63 polyubiquitination is involved in the activation of the canonical pathway (Wertz and Dixit, 2010), and so the effect of preventing this chain formation on the activation of the NF-$\kappa$B pathway was tested. One group has shown that hypercapnia led to increases in polyubiquitination which was blocked by inhibiting the E3 ubiquitin ligase Nedd4-2 (Gwoździńska *et al.*, 2017), which adds K63 linked ubiquitin chains to proteins (Todaro *et al.*, 2017). Cells were pre-incubated at 10% $CO_2$, as done in Figure 3.13 B, and transfected with the vector and K63R mutation at the same time (Figure 3.14). Although there was a significant reduction in NF-$\kappa$B activity with the K63R mutant at 30 ng/ml of TNF-$\alpha$ compared to the vector, the effect of elevated

$CO_2$ was lost on the vector. The fluorescence signal was much stronger than seen in Figure 3.13 B, and so problems with the cell line no longer responding to TNF-$\alpha$ cannot explain this result. As there appeared to be an unknown factor influencing this assay, these results should be considered with caution. Despite this, the data does appear to clearly indicate the importance of K63 polyubiquitination for the activation of the canonical pathway. However, any effects of elevated $CO_2$ on this cannot be concluded from this data due to the loss of the effect of elevated $CO_2$ on the vector. As seen with the K48R ubiquitin mutant transfection, there was not a complete blockade of the NF-$\kappa$B activation. To validate the effect of elevated $CO_2$ on K63R mutant, this assay would need to be repeated.

In summary, the fluorescent signal clearly demonstrated that elevations in $CO_2$ caused a significant reduction in TNF-$\alpha$-induced activation of the canonical pathway. Transfection with mutant ubiquitin has shown that K48 polyubiquitin caused a significant reduction in the cytokine-induced activation of the NF-$\kappa$B pathway. It would also seem likely that blocking K48 polyubiquitin chain formation occluded the effects of elevated $CO_2$. To further confirm this hypothesis, the formation of K48 polyubiquitination would need to be measured at both 5% and 10% $CO_2$ when cells are treated with TNF-$\alpha$.
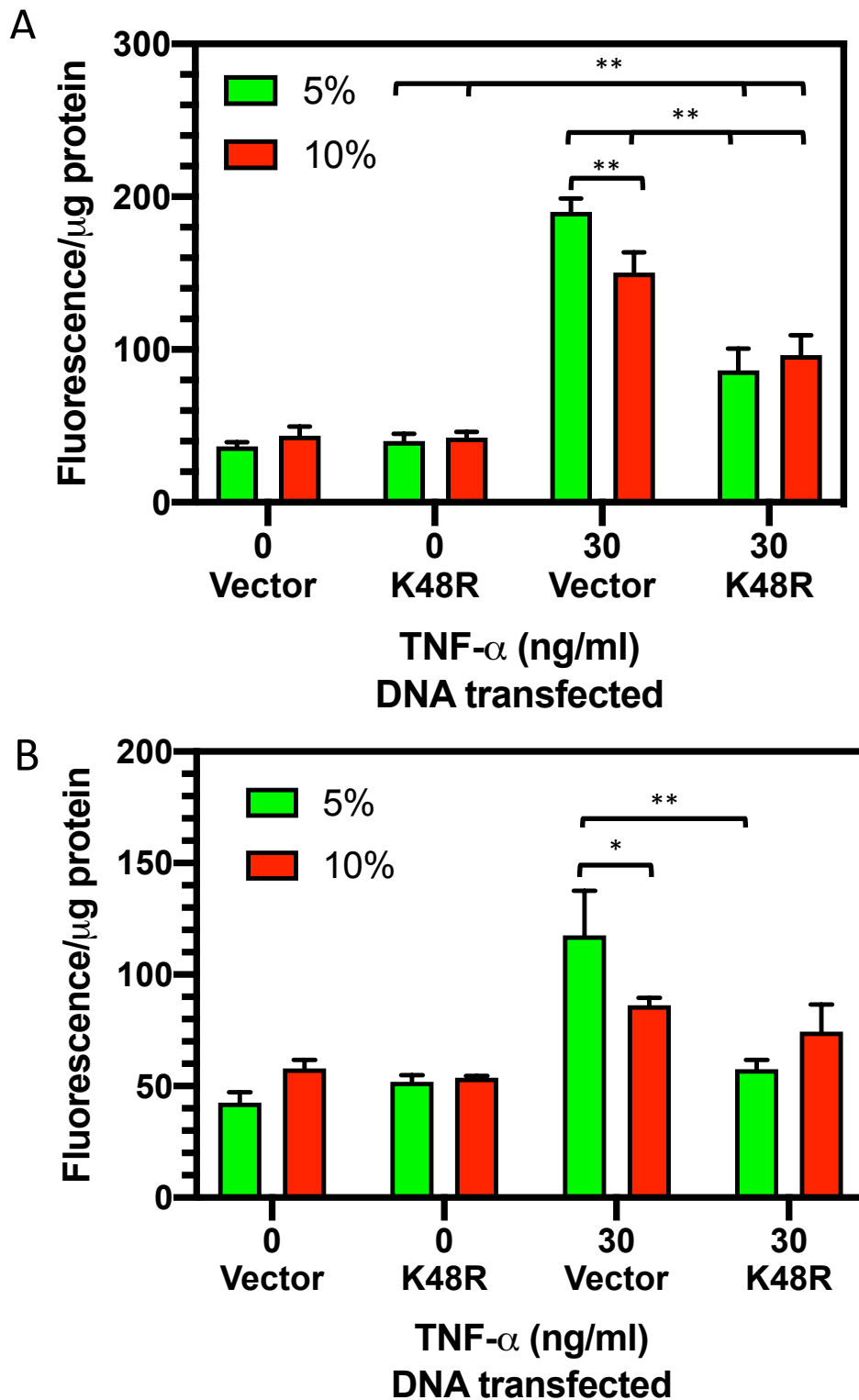
**Figure 3.13**
Transfection of cells with K48R ubiquitin significantly reduced TNF-$\alpha$-induced activation of NF-$\kappa$B. A) Cells were transfected with the pRK5 vector (vector) or K48R mutant (K48R) for 20 hours before treatment with 0 or 30 ng/ml of TNF-$\alpha$ at either 5% or 10% $CO_2$. N=6. B) Same conditions as (A) but with a prior incubation at 10% $CO_2$ when cells were transfected. 0 ng/ml N=3 and 30 ng/ml N=5. Fluorescence was normalised to $\mu$g protein. 'Assay Media' from Table 2.1. Error bars represent standard deviation. T Test * $p < 0.01$ ** $p < 0.001$
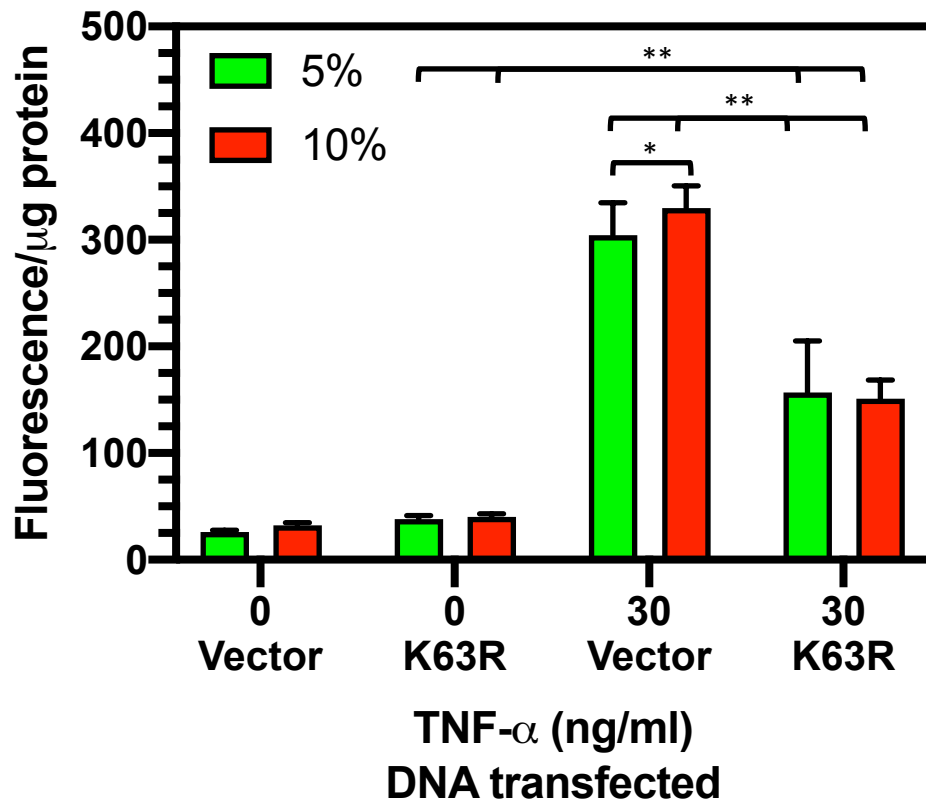
**Figure 3.14**

Transfection with K63R ubiquitin mutant significantly reduced NF-κB activation, but the effect of elevated $CO_2$ was lost. Fluorescence was normalised to μg protein. 'Assay Media' from Table 2.1. Error bars represent standard deviation. 0 ng/ml N=6. 30 ng/ml N=14. T Test * $p < 0.05$ ** $p < 0.0001$

# 4 - Discussion

The hypothesis was to investigate the effect of elevated $CO_2$ levels on the formation of K48 polyubiquitin chains and the effect of this on NF-κB pathway activation in mammalian cells. However, the investigation of this was hindered by the unexpected finding that elevated $CO_2$ increased activation of the pathway, and so potential factors for why this occurred are discussed here. Although measuring the fluorescence signal appeared to resolve this, the reduction in TNF-α-induced activation of NF-κB was lost at the very end of the project. Factors which may have affected the assay results carried out in this project are discussed here. These potential factors include the media pH, cell line, NF-κB stimulus, age of the cells, reporters, detection method for NF-κB activation, media buffer, intracellular pH and transfection efficiency.

## 4.1 Factors potentially influencing the results

As discussed previously, controlling the media pH did not alter the TNF-α-induced increase in Luc signal after treatment with elevated $CO_2$. Similarly, the large error rates seen with luciferase reporter signals (Close *et al.*, 2011) cannot explain the significant increase in activity seen at 10% $CO_2$, as this elevated signal was also seen when measuring fluorescence even when the media pH was also controlled (Figure 3.14). However, the increase in activity seen when measuring the fluorescence was only seen on one transfection assay.

One of the main differences between this study and other investigations into the effect of hypercapnia on NF-κB inflammation are the cell lines used. Most studies have used either the cancer cell line A549 (Abolhassani *et al.*, 2009; Cummins *et al.*, 2010; Oliver *et al.*, 2012; Horie *et al.*, 2016; Masterson *et al.*, 2016; Keogh *et al.*, 2017), inflammatory cells like macrophages (Bidani *et al.*, 1998; Lang *et al.*, 2005; Wang *et al.*, 2010; Gerry and Leake, 2014; Casalino-Matsuda *et al.*, 2015) or epithelial cells (O'Toole *et al.*, 2005; Horie *et al.*, 2016; Masterson *et al.*, 2016) to investigate the NF-κB pathway. Similarly, the most common inflammatory stimulus used is LPS

(Bidani *et al.*, 1998; Laffey *et al.*, 2003; Takeshita *et al.*, 2003; Lang *et al.*, 2005; Cummins *et al.*, 2010; Wang *et al.*, 2010; Oliver *et al.*, 2012; Gerry and Leake, 2014). In this study the HEK 293 derived cell line was used and these do not possess the TLR4 to which LPS binds (Zeuner *et al.*, 2017), and so the cytokine TNF-$\alpha$ was used to activate the canonical pathway. The cell line was chosen as it possessed an NF-$\kappa$B reporter which allowed easy and relatively cheap detection of the canonical pathway activity. Although a large proportion of the evidence on the effects of hypercapnia on the NF-$\kappa$B pathway are effects on LPS-induced activation, there is evidence that hypercapnia also reduces TNF-$\alpha$-induced activation (Cummins *et al.*, 2010; Oliver *et al.*, 2012; Masterson *et al.*, 2016). This rules out the possibility that hypercapnia only affects the unique elements involved in LPS induced activation of the canonical NF-$\kappa$B pathway. Due to the lack of evidence in the literature to prove either way, elevations in $CO_2$ on the NF-$\kappa$B/293/GFP-Luc$^{TM}$ cell line may indeed cause an increase or a decrease in TNF-$\alpha$-induced NF-$\kappa$B activity. Unfortunately, investigations into a different cell line (U251-NF-$\kappa$B-GFP-Luc) were impeded due to problems with the reporter not responding to TNF-$\alpha$ treatment, and so a unique response in this specific cell line could not be fully tested. However, although the Luc signal repeatedly showed hypercapnia caused a significant increase in activity, the fluorescence signal only indicated this once. Therefore, it would seem likely that 10% $CO_2$ does reduce NF-$\kappa$B inflammation in the NF-$\kappa$B/293/GFP-Luc$^{TM}$ cell line.

Another major factor differentiating this project from previous studies, are the methods for detecting NF-$\kappa$B activation. This study only used the reporter output as an indication of pathway activation and while other studies have used reporter cell lines, they measured other factors like IL-8 secretion or nuclear translocation of NF-$\kappa$B subunits to verify canonical activation (Cummins *et al.*, 2010; Horie *et al.*, 2016). The loss of the effect of elevated $CO_2$ when measuring the fluorescence signal in Figure 3.14 could indicate that the reporter within this cell line was not stable. However, the NF-$\kappa$B/293/GFP-Luc$^{TM}$ cell line was transduced with the reporter DNA using a HIV-based lentivector packaged into pseudoviral particle. This method of transduction allows for genomic integration of DNA and provides stable expression

of the vector (Mendenhall *et al.*, 2012). By using a stably-integrated reporter cell line this rules out the possibility that the hypercapnia condition was impacting on the reporter transfection efficiency, of course this cannot be said of the K48R and K63R ubiquitin mutants which were transfected into the cell line at elevated $CO_2$. Therefore, the inconsistent results would seem unlikely to be caused by an unstable reporter transduction; and the loss of the effect of elevated $CO_2$ was only seen once when measuring the fluorescence signal.

Cells used in the assays were passaged no greater than 18 times to minimise the risk of reporter mutation. A mutation within the cell line could have occurred during the freezing and thawing process or at any point during the growth and maintenance of the cells. If there was a problem with the reporter due to a mutation, there would most likely be no or a minimal signal detected as seen with the U251-NF-κB-GFP-Luc cells. Across independent assays both the raw Luc and Fluorescence signals varied widely, a factor which cannot be explained by cell count as all signals were normalised to protein content. This could hint to an instability to the reporter system within this cell line. To verify the effectiveness of using the reporter as an accurate output of canonical activation, the translocation of the NF-κB subunits to the nucleus or measuring the cytokine secretion using an ELISA could be carried out in conjunction with measuring the reporter signal. This would also help to validate that elevated $CO_2$ does cause a reduction in NF-κB activity within the NF-κB/293/GFP-Luc[TM] cell line.

The media pH was controlled by altering the level of sodium bicarbonate added to the media. Although other studies have used this to control the media pH (Takeshita *et al.*, 2003; Cummins *et al.*, 2010; Oliver *et al.*, 2012; Horie *et al.*, 2016), many other studies used hydrochloric acid to reduce media pH in the normocapnia condition (Takeshita *et al.*, 2003; O'Toole *et al.*, 2005; Abolhassani *et al.*, 2009; Cummins *et al.*, 2010; Wang *et al.*, 2010; Oliver *et al.*, 2012; Gerry and Leake, 2014). There were difficulties producing consistent media pH levels when hydrochloric acid was used (data not shown), and so sodium bicarbonate was chosen to alter media pH as this produced stable and reproducible pH results. When there are elevations in $CO_2$ there

are increases in bicarbonate as well as H$^+$ (Figure 1.1). With increasing $CO_2$ levels the more sodium bicarbonate added to media, and so the bicarbonate levels would have been quite different across the 5% and 10% $CO_2$ conditions. Therefore, differences seen between the 5% and 10% $CO_2$ may be caused by or contributed by difference in bicarbonate levels. To test if the bicarbonate was affecting the NF-κB activation, a different buffering system could be used or potentially by altering the HEPES concentration across the 5% and 10% media.

The most likely cause for the loss of the effect of elevated $CO_2$, are factors which were not controlled consistently. It is possible that the $CO_2$ was not tightly controlled within the 10% $CO_2$ incubator, and the levels were not consistently held across experiments. The 10% $CO_2$ incubator used for the assays however was newly purchased and this would seem an unlikely cause. Although the extracellular pH was controlled across experiments, the intracellular pH levels were never measured and so may have varied across assays. The intracellular pH could be controlled by treatment of cells with propionic acid (Cook, 2012); however it has previously been shown that the intracellular pH was not significantly altered at 10% $CO_2$ (Cummins *et al.*, 2010). Another factor potentially influencing the results was the sonication of the cell samples. To collect the samples for sonication, each well needed to be scraped to remove adhered cells from the plate and then collected. If there were many samples from 1 plate the wells may have equilibrated to ambient $CO_2$ condition by the time the cells were collected and then lysed. Sonication of each sample was also quite a time consuming method and the differences in the time that samples were stored on ice may have affected the breakdown of the Luciferase or GFP. Differences in these times across assays may help to explain why the signal varied so widely between independent assays. To reduce the differences in time across samples, a lysis buffer could be used which did not react with the Bradford Reagent or another reagent that allows for sample protein concentration estimation. Alternatively, using a dual-luciferase reporter (express the NF-κB reporter and a constitutively active *Renilla* luciferase reporter) as an internal control for transfection efficiency and to allow detection of any off-target changes to the reporter activity (Paguio *et al.*, 2010). However this also has its downfalls, with evidence indicating that cellular factors can

alter the *Renilla* reporter activity and reduce its efficacy of being a control reporter (Zhang *et al.*, 2017).

Another factor which could have impacted the results of the assays are problems with the transfection process. The transfection efficiency was never determined in the experiments comparing the ubiquitin mutants to the vector controls, and so there could have been vast differences in transfection efficiencies across experiments. If one assay had much lower transfection efficiency there would be a much higher background activation when stimulated with TNF-$\alpha$. As the results became inconsistent once the cells were treated with elevated $CO_2$ conditions at the time of transfection, it is possible the 10% $CO_2$ treatment impacted on the efficiency of transfection. Alternatively, repeated freezing and thawing of the vector and K48R ubiquitin mutant may have reduced the DNA quality. Transfection with the pRK5 vector alone reduced the TNF-$\alpha$ induced activation of NF-$\kappa$B (data not shown), and so the increase in activity seen at 10% $CO_2$ in Figure 3.14 could be attributed to lower transfection efficiency in these samples.

Due to the complexity of whole cell systems and the many aspects which can influence assay results, it can be difficult to pinpoint why one study appears to contradict another. The inconsistencies within the literature, as discussed in the introduction, just highlights the complex nature of hypercapnia on NF-$\kappa$B inflammation *in vitro* and *in vivo*.

## 4.2 pH or $CO_2$?

There is compelling evidence that larger reductions in media pH causes a significant attenuation in NF-$\kappa$B activation after TNF-$\alpha$ treatment in the NF-$\kappa$B/293/GFP-Luc$^{TM}$ cell line (Figure 3.5). Smaller reductions in pH did not seem to cause a significant reduction in activity at either 5% or 10% $CO_2$ (Figure 3.6). This like other studies (Wang *et al.*, 2010), would indicate that the alteration in activity caused by pH and $CO_2$ are via different mechanisms. Indeed, a reduction in pH would increase the number of $H^+$ which could then interact with negatively charged amino acids and

alter the charge and function of proteins; while increases in $CO_2$ may alter protein functionality through carbamylation of lysine residues. Once the media pH was controlled, although there were significant changes in activity, the alterations were relatively small in comparison to previous studies which found a 4-5 fold reduction in NF-κB activity at 10% $CO_2$ (Cummins *et al.*, 2010). This may be caused by the NF-κB/293/GFP-Luc<sup>TM</sup> cell line having a smaller response to hypercapnia than other cell lines tested, the large reduction seen by Cummins et al. could be caused by a combination of both increased $CO_2$ and reduced pH, or that the method used in this study was much less sensitive at detecting changes to activity. From the evidence in this study it would appear that both pH and $CO_2$ play a role in regulating the canonical pathway within the NF-κB/293/GFP-Luc<sup>TM</sup> cell line.

## 4.3 Is K48 carbamylation responsible for hypercapnia-induced attenuation of the canonical pathway?

The evidence within this study would clearly indicate that the K48 polyubiquitin chains are important for the activation of the canonical pathway; something which is already known (Wertz and Dixit, 2010). However, the hypothesis stated carbamylation of K48 prevented the formation of K48 polyubiquitin chains, and by preventing the formation of these chains occluded the effects of hypercapnia (Figure 3.13 A). The fact that hypercapnia did not cause any increase in the NF-κB activity reduction, would mean that the K48R mutation blocked the mechanism by which hypercapnia acts or that it is a more powerful shutdown of the pathway and masks the effect of hypercapnia. Although K48R occluding the effect of hypercapnia does not conclusively indicate that this is the mechanism by which hypercapnia is acting, it does provide compelling evidence.

## 4.4 Conclusions

Overall this study has shown that both $CO_2$ and pH are able to cause reductions to the canonical NF-κB pathway within the NF-κB/293/GFP-Luc$^{TM}$ cell line. However, the repeated initial findings which indicated hypercapnic acidosis increased NF-κB activity, reflects the conflicting evidence within the literature and highlights there are still aspects of hypercapnic acidosis effects on inflammation which are unknown. Despite this, this study has demonstrated that mutating the ubiquitin lysine to an arginine at residue 48, significantly reduces the activation of the canonical pathway. There is compelling evidence that carbamylation at K48 of ubiquitin reduces the activation of the pathway, due to the effects of hypercapnia being occluded by K48R ubiquitin mutant.

# 5 - Future Work

Firstly the methodology of these assays would need to be tested further to rule out the factors mentioned within the discussion section. For instance, to verify the reporter accuracy for measuring activity could be done by also detecting NF-κB subunit translocation to the nucleus by Western Blotting. Alternatively, the short half-life of copGFP within the reporter cell line would allow the tracking of real-time GFP imaging and quantification of activity over a time course. Similarly, due to the unknown involvement of bicarbonate in this reaction a different buffering system could be tested, for instance using different HEPES concentrations across the 5% and 10% $CO_2$ media.

Once the experimental design had been sorted, then the effect of mutating the other ubiquitin lysine residues (K6, K11, K27, K29, K33 and K63) on the activation of the NF-κB pathway could be tested. The effect of hypercapnia on these mutants would also be tested to see if carbamylation occurs on all ubiquitin lysine residues, and to see if all chain formations are hindered by hypercapnic conditions. To verify if K48 or any other polyubiquitin chain formation is attenuated under hypercapnic conditions, then a Western Blot comparing the level of polyubiquitination that occurs at 5% and 10% after TNF-α stimulation could be carried out. Specific antibodies for the different polyubiquitin chain would be used to test the effect of hypercapnia across all polyubiquitin chains.

Assuming the central hypothesis is correct, the larger reduction in activity after TNF-α treatment seen by flooding the system with K48R ubiquitin mutants compared to 10% $CO_2$ treatment alone, could indicate that carbamylation does not occur to all ubiquitin molecules within the cell. If this was the case then treatment with higher levels of $CO_2$ would cause even greater reductions in canonical activation, and previous studies have shown larger effects at higher $CO_2$ concentrations (Lang *et al.*, 2005). Therefore, the effect of 15% and 20% $CO_2$ on the shutdown of the NF-κB pathway, and their effects on cells transfected with K48R ubiquitin mutant could also be tested. However, the physiological significance of such high $CO_2$ is questionable.

Another aspect of the project which could also be investigated would be the effect of hypercapnia on the non-canonical pathway. The non-canonical pathway also requires K48 polyubiquitination of the p100 subunit, which signals a protein modification converting it into the active non-canonical NF-κB subunit, p52 (Wertz and Dixit, 2010). If the original hypothesis is correct about K48 ubiquitin carbamylation, it may help to explain the reductions to the non-canonical pathway activity under hypercapnic conditions (Oliver *et al.*, 2012; Keogh *et al.*, 2017).

Finally, it would be interesting to test some of these ideas within an animal model, to see if these effects are reflected *in vivo* and not just artefacts of *in vitro* experiments. Unknown elements within other systems may be at play that alter the overall effect of hypercapnic acidosis, and the physiological relevance of some of these factors may be less important.

# 6 - Bibliography

Abolhassani, M. *et al.* (2009) 'Carbon dioxide inhalation causes pulmonary inflammation.', *American journal of physiology. Lung cellular and molecular physiology*. doi: 10.1152/ajplung.90460.2008.

Akutsu, M., Dikic, I. and Bremm, A. (2016) 'Ubiquitin chain diversity at a glance', *Journal of Cell Science*. doi: 10.1242/jcs.183954.

Beerling, D. J. and Berner, R. A. (2005) 'Feedbacks and the coevolution of plants and atmospheric CO2', *Proceedings of the National Academy of Sciences*. doi: 10.1073/pnas.0408724102.

Bidani, A. *et al.* (1998) 'Evidence for pH sensitivity of tumor necrosis factor-α release by alveolar macrophages', *Lung*. doi: 10.1007/PL00007593.

Bohr, C., Hasselbalch, K. and Krogh, A. (1904) 'About a new biological relation of high importance that the blood carbonic acid tension exercises on its oxygen binding', *Skandinavisches Archiv Fur Physiologie*. , 16, pp. 402–412.

Casalino-Matsuda, S. M. *et al.* (2015) 'Hypercapnia Inhibits Autophagy and Bacterial Killing in Human Macrophages by Increasing Expression of Bcl-2 and Bcl-xL', *The Journal of Immunology*. doi: 10.4049/jimmunol.1500150.

Caso, G. *et al.* (2005) 'Response of protein synthesis to hypercapnia in rats: Independent effects of acidosis and hypothermia', *Metabolism: Clinical and Experimental*. doi: 10.1016/j.metabol.2005.01.026.

Chau, V. *et al.* (1989) 'A multiubiquitin chain is confined to specific lysine in a targeted short-lived protein', *Science*. doi: 10.1126/science.2538923.

Chiao, P. J., Miyamoto, S. and Verma, I. M. (1994) 'Autoregulation of I kappa B alpha activity.', *Proceedings of the National Academy of Sciences*. doi: 10.1073/pnas.91.1.28.

Christiansen, J., Douglas, C. G. and Haldane, J. S. (1914) 'The absorption and dissociation of carbon dioxide by human blood', *The Journal of Physiology*. doi: 10.1113/jphysiol.1914.sp001659.

Close, D. M. *et al.* (2011) 'Comparison of human optimized bacterial luciferase, firefly luciferase, and green fluorescent protein for continuous imaging of cell culture and animal models', *Journal of Biomedical Optics*. doi:

10.1117/1.3564910.

Contreras, M. *et al.* (2012) 'Hypercapnic acidosis attenuates ventilation-induced lung injury by a nuclear factor-κB-dependent mechanism', *Critical Care Medicine*. doi: 10.1097/CCM.0b013e318258f8b4.

Cook, Z. (2012) *The Influence of Carbon Dioxide on Cellular Cyclic Adenosine Monophosphate*. Durham University.

Cummins, E. P. *et al.* (2010) 'NF- B Links CO2 Sensing to Innate Immunity and Inflammation in Mammalian Cells', *The Journal of Immunology*. doi: 10.4049/jimmunol.1000701.

Cummins, E. P. *et al.* (2014) 'Carbon dioxide-sensing in organisms and its implications for human disease', *Cellular and Molecular Life Sciences*. doi: 10.1007/s00018-013-1470-6.

Curley, G., Laffey, J. G. and Kavanagh, B. P. (2010) 'Bench-to-bedside review: Carbon dioxide', *Critical Care*. doi: 10.1186/cc8926.

Devaney, J. *et al.* (2013) 'Inhibition of pulmonary nuclear factor kappa-B decreases the severity of acute Escherichia coli pneumonia but worsens prolonged pneumonia', *Critical Care*. doi: 10.1186/cc12696.

Doerr, C. H. *et al.* (2005) 'Hypercapnic acidosis impairs plasma membrane wound reseating in ventilator-injured lungs', *American Journal of Respiratory and Critical Care Medicine*. doi: 10.1164/rccm.200309-1223OC.

Ducrest, A.-L. (2002) 'Detection of promoter activity by flow cytometric analysis of GFP reporter expression', *Nucleic Acids Research*. doi: 10.1093/nar/gnf064.

Dynek, J. N. *et al.* (2010) 'C-IAP1 and UbcH5 promote K11-linked polyubiquitination of RIP1 in TNF signalling', *EMBO Journal*. doi: 10.1038/emboj.2010.300.

Emmerich, C. H. *et al.* (2013) 'Activation of the canonical IKK complex by K63/M1-linked hybrid ubiquitin chains', *Proceedings of the National Academy of Sciences*. doi: 10.1073/pnas.1314715110.

Finley, D. *et al.* (1994) 'Inhibition of proteolysis and cell cycle progression in a multiubiquitination-deficient yeast mutant.', *Molecular and Cellular Biology*. doi: 10.1128/mcb.14.8.5501.

Foecking, M. K. and Hofstetter, H. (1986) 'Powerful and versatile enhancer-promoter unit for mammalian expression vectors', *Gene*. doi: 10.1016/0378-

1119(86)90137-X.

Gates, K. L. *et al.* (2013) 'Hypercapnia impairs lung neutrophil function and increases mortality in murine Pseudomonas pneumonia', *American Journal of Respiratory Cell and Molecular Biology*. doi: 10.1165/rcmb.2012-0487OC.

Gerry, A. B. and Leake, D. S. (2014) 'Effect of low extracellular pH on NF-κB activation in macrophages', *Atherosclerosis*. doi: 10.1016/j.atherosclerosis.2014.01.014.

Gwoździńska, P. *et al.* (2017) 'Hypercapnia impairs ENaC cell surface stability by promoting phosphorylation, polyubiquitination and endocytosis of β-ENac in a human alveolar epithelial cell line', *Frontiers in Immunology*. doi: 10.3389/fimmu.2017.00591.

Hayden, M. S. and Ghosh, S. (2012) 'NF-κB, the first quarter-century: Remarkable progress and outstanding questions', *Genes and Development*. doi: 10.1101/gad.183434.111.

Higgins, B. D. *et al.* (2009) 'Differential effects of buffered hypercapnia versus hypercapnic acidosis on shock and lung injury induced by systemic sepsis', *Anesthesiology*. doi: 10.1097/ALN.0b013e3181ba3c11.

Horie, S. *et al.* (2016) 'Hypercapnic acidosis attenuates pulmonary epithelial stretch-induced injury via inhibition of the canonical NF-kappaB pathway.', *Intensive care medicine experimental*. doi: 10.1186/s40635-016-0081-6.

Hsia, C. C. W. (2002) 'Respiratory Function of Hemoglobin', *New England Journal of Medicine*. doi: 10.1056/nejm199801223380407.

Huckstepp, R. T. R. *et al.* (2010) 'Connexin hemichannel-mediated CO2-dependent release of ATP in the medulla oblongata contributes to central respiratory chemosensitivity', *Journal of Physiology*. doi: 10.1113/jphysiol.2010.192088.

Ito, Y. and Ushitora, H. (2006) 'Trapping of carbamic acid species with (trimethylsilyl)diazomethane', *Tetrahedron*. doi: 10.1016/j.tet.2005.09.116.

Iwai, K. (2012) 'Diverse ubiquitin signaling in NF-κB activation', *Trends in Cell Biology*. doi: 10.1016/j.tcb.2012.04.001.

Iwai, K. (2014) 'Diverse roles of the ubiquitin system in NF-κB activation', *Biochimica et Biophysica Acta - Molecular Cell Research*. doi: 10.1016/j.bbamcr.2013.03.011.

Jimenez-Morales, D. *et al.* (2014) 'Lysine carboxylation: Unveiling a spontaneous post-translational modification', *Acta Crystallographica Section D: Biological Crystallography*. doi: 10.1107/S139900471302364X.

Keogh, C. E. *et al.* (2017) 'Carbon dioxide-dependent regulation of NF-κB family members RelB and p100 gives molecular insight into CO2-dependent immune regulation', *Journal of Biological Chemistry*. doi: 10.1074/jbc.M116.755090.

Laffey, J. G. *et al.* (2003) 'Hypercapnic Acidosis Attenuates Endotoxin-induced Acute Lung Injury', *American Journal of Respiratory and Critical Care Medicine*. doi: 10.1164/rccm.200205-394oc.

Lang, C. J. *et al.* (2005) ' Effect of CO 2 on LPS-induced cytokine responses in rat alveolar macrophages ', *American Journal of Physiology-Lung Cellular and Molecular Physiology*. doi: 10.1152/ajplung.00394.2004.

Lee, E. G. *et al.* (2000) 'Failure to regulate TNF-induced NF-κB and cell death responses in A20-deficient mice', *Science*. doi: 10.1126/science.289.5488.2350.

Lim KL, Chew KC, Tan JM, Wang C, Chung KK, Zhang Y, Tanaka Y, Smith W, Engelender S, Ross CA, Dawson VL, D. T. (2005) 'Parkin Mediates Nonclassical, Proteasomal-Independent Ubiquitination of Synphilin-1: Implications for Lewy Body Formation', *Journal of Neuroscience*. doi: 10.1523/JNEUROSCI.4474-04.2005.

Lindskog, S. and Coleman, J. E. (1973) 'The catalytic mechanism of carbonic anhydrase', *Proceedings of the National Academy of Sciences of the United States of America*. doi: 10.1073/pnas.70.9.2505.

Linthwaite, V. L. *et al.* (2018) 'The identification of carbon dioxide mediated protein post-translational modifications', *Nature Communications*. doi: 10.1038/s41467-018-05475-z.

Lorimer, G. H. (1979) 'Evidence for the existence of discrete activator and substrate sites for CO2 on ribulose-1,5-bisphosphate carboxylase.', *Journal of Biological Chemistry*.

Lorimer, G. H., Badger, M. R. and Andrews, T. J. (1976) 'The Activation of Ribulose-1,5-bisphosphate Carboxylase by Carbon Dioxide and Magnesium Ions. Equilibria, Kinetics, a Suggested Mechanism, and Physiological implications',

*Biochemistry*. doi: 10.1021/bi00648a012.

Lorimer, G. H. and Miziorko, H. M. (1980) 'Carbamate Formation on theε-Amino Group of a Lysyl Residue as the Basis for the Activation of Ribulosebisphosphate Carboxylase by Carbon Dioxide and Magnesium(2+)', *Biochemistry*. doi: 10.1021/bi00564a027.

Masterson, C. *et al.* (2016) 'Effects and Mechanisms by Which Hypercapnic Acidosis Inhibits Sepsis-Induced Canonical Nuclear Factor-κB Signaling in the Lung', *Critical Care Medicine*. doi: 10.1097/CCM.0000000000001376.

Matthew, J. B. *et al.* (1977) 'Quantitative determination of carbamino adducts of α and β chains in human adult hemoglobin in presence and absence of carbon monoxide and 2,3 diphosphoglycerate', *Journal of Biological Chemistry*.

McGee, M. (2015) *CO2 Earth*. Available at: https://www.co2.earth/annual-co2 (Accessed: 3 January 2020).

Meigh, L. *et al.* (2013) 'CO2 directly modulates connexin 26 by formation of carbamate bridges between subunits', *eLife*. doi: 10.7554/elife.01213.

Mendenhall, A. *et al.* (2012) 'Packaging HIV- or FIV-based Lentivector Expression Constructs & Transduction of VSV-G Pseudotyped Viral Particles', *Journal of Visualized Experiments*. doi: 10.3791/3171.

Mitchell, S., Vargas, J. and Hoffmann, A. (2016) 'Signaling via the NFκB system', *Wiley Interdisciplinary Reviews: Systems Biology and Medicine*. doi: 10.1002/wsbm.1331.

Muthu, V. *et al.* (2017) '"Permissive" hypercapnia in ARDS: is it passé?', *Intensive Care Medicine*. doi: 10.1007/s00134-017-4794-0.

Newton, K. *et al.* (2008) 'Ubiquitin Chain Editing Revealed by Polyubiquitin Linkage-Specific Antibodies', *Cell*. doi: 10.1016/j.cell.2008.07.039.

Nin, N. *et al.* (2017) 'Severe hypercapnia and outcome of mechanically ventilated patients with moderate or severe acute respiratory distress syndrome', *Intensive Care Medicine*. doi: 10.1007/s00134-016-4611-1.

O'Croinin, D. F. *et al.* (2008) 'Sustained hypercapnic acidosis during pulmonary infection increases bacterial load and worsens lung injury', *Critical Care Medicine*. doi: 10.1097/CCM.0b013e31817d1b59.

O'Toole, D. *et al.* (2005) 'Low pH and Helicobacter pylori increase nuclear factor

kappa B binding in gastric epithelial cells: A common pathway for epithelial cell injury?', *Journal of Cellular Biochemistry*. doi: 10.1002/jcb.20539.

O'Toole, D. *et al.* (2009) 'Hypercapnic acidosis attenuates pulmonary epithelial wound repair by an NF-κB dependent mechanism', *Thorax*. doi: 10.1136/thx.2008.110304.

Oliver, K. M. *et al.* (2012) 'Hypercapnia induces cleavage and nuclear localization of RelB protein, giving insight into $CO_2$ sensing and signaling', *Journal of Biological Chemistry*. doi: 10.1074/jbc.M112.347971.

Paguio, A. *et al.* (2010) 'Improved dual-luciferase reporter assays for nuclear receptors', *Current Chemical Genomics*. doi: 10.2174/1875397301004010043.

Pahl, H. L. (1999) 'Activators and target genes of Rel/NF-κB transcription factors', *Oncogene*. doi: 10.1038/sj.onc.1203239.

Pronobis, M. I., Deuitch, N. and Peifer, M. (2016) 'The Miraprep: A protocol that uses a Miniprep kit and provides Maxiprep yields', *PLoS ONE*. doi: 10.1371/journal.pone.0160509.

Putnam, R. W., Filosa, J. A. and Ritucci, N. A. (2004) ' Cellular mechanisms involved in $CO_2$ and acid signaling in chemosensitive neurons ', *American Journal of Physiology-Cell Physiology*. doi: 10.1152/ajpcell.00282.2004.

Rodova, M. *et al.* (2013) 'CMV promoter is repressed by p53 and activated by JNK pathway', *Plasmid*. doi: 10.1016/j.plasmid.2013.01.004.

Skaug, B., Jiang, X. and Chen, Z. J. (2009) 'The Role of Ubiquitin in NF-κB Regulatory Pathways', *Annual Review of Biochemistry*. doi: 10.1146/annurev.biochem.78.070907.102750.

Spence, J. *et al.* (2015) 'A ubiquitin mutant with specific defects in DNA repair and multiubiquitination.', *Molecular and Cellular Biology*. doi: 10.1128/mcb.15.3.1265.

Sun, S. C. (2010) 'CYLD: A tumor suppressor deubiquitinase regulating NF-B activation and diverse biological processes', *Cell Death and Differentiation*. doi: 10.1038/cdd.2009.43.

Sun, S. C. (2011) 'Non-canonical NF-κB signaling pathway', *Cell Research*. doi: 10.1038/cr.2010.177.

Takeshita, K. *et al.* (2003) 'Hypercapnic acidosis attenuates endotoxin-induced

nuclear factor-κB activation', *American Journal of Respiratory Cell and Molecular Biology*. doi: 10.1165/rcmb.2002-0126OC.

Taylor, C. T. and Cummins, E. P. (2011) 'Regulation of gene expression by carbon dioxide', *Journal of Physiology*. doi: 10.1113/jphysiol.2010.201467.

Taylor, T. C. and Andersson, I. (1996) 'Structural transitions during activation and ligand binding in hexadecameric Rubisco inferred from the crystal structure of the activated unliganded spinach enzyme', *Nature Structural Biology*. doi: 10.1038/nsb0196-95.

Terrier, P. and Douglas, D. J. (2010) 'Carbamino group formation with peptides and proteins studied by mass spectrometry', *Journal of the American Society for Mass Spectrometry*. doi: 10.1016/j.jasms.2010.05.008.

TheAcuteRespiratoryDistressSyndromeNetwork (2000) 'Ventilation with lower tidal volumes as compared with traditional tidal volumes for acute lung injury and the acute respiratory distress syndrome. The Acute Respiratory Distress Syndrome Network', *N Engl J Med*. doi: 10.1056/nejm200005043421801.

Thompson, J. F., Hayes, L. S. and Lloyd, D. B. (1991) 'Modulation of firefly luciferase stability and impact on studies of gene regulation', *Gene*. doi: 10.1016/0378-1119(91)90270-L.

Todaro, D. R. *et al.* (2017) 'The mechanism of neural precursor cell expressed developmentally down-regulated 4-2 (Nedd4-2)/NEDD4L-catalyzed polyubiquitin chain assembly', *Journal of Biological Chemistry*. doi: 10.1074/jbc.M117.817882.

Tokunaga, F. *et al.* (2009) 'Involvement of linear polyubiquitylation of NEMO in NF-κB activation', *Nature Cell Biology*. Nature Publishing Group, 11, p. 123. Available at: https://doi.org/10.1038/ncb1821.

Wang, N. *et al.* (2010) 'Elevated CO2 selectively inhibits interleukin-6 and tumor necrosis factor expression and decreases phagocytosis in the macrophage.', *The FASEB journal : official publication of the Federation of American Societies for Experimental Biology*. doi: 10.1096/fj.09-136895.

Wertz, I. E. and Dixit, V. M. (2010) 'Signaling to NF-kappaB: regulation by ubiquitination.', *Cold Spring Harbor perspectives in biology*.

Yang, W. *et al.* (2015) 'Comparison of the effects of moderate and severe

hypercapnic acidosis on ventilation-induced lung injury', *BMC Anesthesiology*. doi: 10.1186/s12871-015-0050-8.

Yokota, A. (2017) 'Revisiting RuBisCO', *Bioscience, Biotechnology and Biochemistry*. doi: 10.1080/09168451.2017.1379350.

Zeuner, M. T. *et al.* (2017) 'Development and Characterisation of a Novel NF- κ B Reporter Cell Line for Investigation of Neuroinflammation', *Mediators of Inflammation*. doi: 10.1155/2017/6209865.

Zhang, D. *et al.* (2017) 'False responses of Renilla luciferase reporter control to nuclear receptor TR4', *Molecular and Cellular Biochemistry*. doi: 10.1007/s11010-017-2961-9.

Zhou, W. *et al.* (2018) 'MicroRNA-21 down-regulates inflammation and inhibits periodontitis', *Molecular Immunology*. doi: 10.1016/j.molimm.2018.05.008.